THE SEARCH FOR THE WEAK (1.14 MEV.) GAMMA RAY OF CADMIUM ^{115m} AND A LITERATURE RESEARCH ON Tc^{96}, Te^{119} AND Te^{121}

Thesis for the Degree of M. S. in Physics

MICHIGAN STATE UNIVERSITY

RICARDO S. PASCUAL, JR.

1962

ABSTRACT

THE SEARCH FOR THE WEAK (1.14 Mev.) GAMMA RAY OF CADMIUM^{115m} AND A LITERATURE RESEARCH ON Tc^{96}, Te^{119} AND Te^{121}.

by Ricardo S. Pascual, Jr.

To furnish an additional verification of the previously reported 1.14-Mev. gamma ray from Cadmium^{115m}, the spectrum of Sodium^{22} (the 1.28-Mev. gamma) and Scandium^{46} (the 0.88-Mev. gamma) were subtracted from the scintillation spectrum of the Cadmium isotope obtained with the 256-Channel Analyzer. The resulting spectral neighborhood showed a full-energy peak at 1.14 Mev.

In addition, some of the latest information and estimates on Tc^{96}, Te^{119} and Te^{121} were summarized to aid in future experiments on these isotopes. Furthermore, some theoretical predictions on the internal conversion coefficients of these isotopes were made for comparison purposes with the observations of future experiments on these same isotopes.

THE SEARCH FOR THE WEAK (1.14 Mev.) GAMMA RAY OF CADMIUM^{115m}

AND

A LITERATURE RESEARCH ON Tc^{96}, Te^{119} AND Te^{121}.

by Ricardo S. Pascual, Jr.

A Thesis

Submitted to
the College of Science and Arts
Michigan State University of Agriculture
and Applied Sciences in partial fulfillment
of the requirements for the degree of

MASTER OF SCIENCE

Department of Physics

1962

Approved: 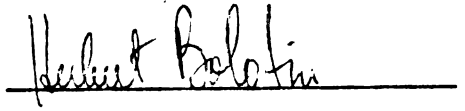

ACKNOWLEDGEMENTS

I am greatly indebted to Dr. William Kelly who suggested the problem and assisted in the actual investigation through his proposal of the subtraction technique; and to Dr. Herbert Bolotin who later assumed a similar task. I am very grateful to Dr. Bolotin for his guidance and help to make the completion of the research possible, and for his painstaking efforts in checking the manuscript.

TABLE OF CONTENTS

- o O o -

LIST OF TABLES

LIST OF FIGURES

INTRODUCTION

RADIOACTIVITY:

Radioactivity is the emission of energetic particles (alpha or beta particles) or electromagnetic radiations (gamma rays) from unstable nuclei. The only means of detecting and measuring these emissions is through the observable effects of their interaction with electromagnetic fields and matter. One of these means is the Scintillation Technique which is based on the effects of interaction of the radioactive emission with special substances known as "phosphors"; this will be explained in necessary detail in the later portions of this paper.

For this particular presentation, it is necessary to discuss only two types of radioactive emissions:

(1) Beta Particles:

A number of experiments in the past have proven that this type of emission is composed of fast-moving electrons; the only distinction from the earlier-defined electron be- the fact that these energetic particles originate from the nucleus instead of the extranuclear electronic orbits of the atom. There are no electrons existing as such in the nucleus. An electron, however, may be formed and ejected from the nucleus by means of a neutron decay into a proton and an electron (accompanied by a neutrino). The electrically neutral neutrino with a negligible rest mass is emitted to conserve the energy and the angular momentum in this neutron decay process. Beta particle emission is an isobaric process, producing a daughter nucleus which

has the same mass number (the nucleon number; i.e., the total number of protons and neutrons in the nucleus), but having an atomic number (i.e., the number of protons or the number of atomic electrons) which is one more than that of the parent nucleus. When the transition is from the ground state (state of lowest excitation energy) of the parent nucleus to the ground state of the daughter nucleus, the energy available for the beta decay comes from the difference in mass of the nuclei involved.

One method for determining the velocities of these particles (hence their energies) is by the measurement of the radii of curvature of their paths in a uniform magnetic field of constant intensity (perpendicular to the beta beam). By equating the Lorentz force to the Centrifugal force, the velocities can be obtained as a function of the known magnetic field intensity or the radius of curvature. This then, may result in a velocity or momentum distribution of the beta particles from the radioactive source.

The resulting momentum (or energy) spectrum from a beta disintegration is distinct from other types of spectra characteristic of the same atom (viz., optical , characteristic X-rays, etc.); in that, it is a continuous one. The other characteristic spectra are line spectra. The continuous beta spectrum exhibits a "preferred" energy (the energy possessed by the greatest number) and a maximum energy limit. This maximum limit or "end-point energy" is interpreted as the energy released in this particular radioactive disintegration. A typical beta spectrum is shown in Fig. 1.

Oftentimes, the continuous beta spectrum is superimposed on a "sharp line" spectrum which is an indication of the presence of electrons which have been ejected from the extranuclear orbits of the atom. These internal conversion (IC) electrons are emitted as a result of the interaction

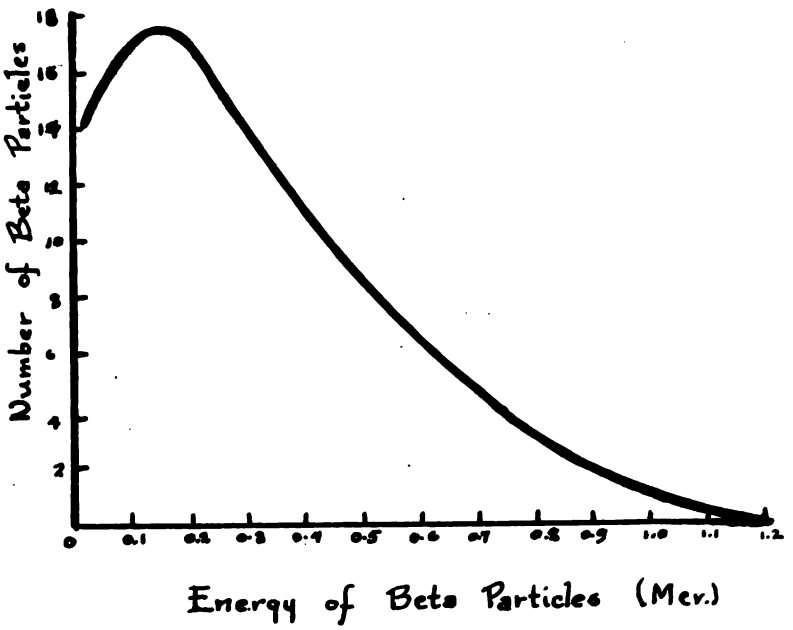

Fig. 1 Energy Distribution among the Beta-Particles of Radium E.

of the orbital electrons with the electromagnetic field of their own nucleus. The ejection of an orbital electron leaves the extranuclear portion of the atom in an excited state. There are a number of ways by which this instability could be removed by the atom itself. In one, the remaining orbital electrons may rearrange to fill the vacancy created by the IC electron (inner orbit) and in so doing, emit fluorescent X-rays. Each X-ray photon represents the energy released in a particular electronic transition. In this case, the energy of the X-ray photon is the difference between the binding energies of the initial and final states of the particular electron which participated in the rearrangement to fill the vacancy left by the IC electron.

Another possibility by which the atom may return to stability is the so-called Auger effect. Here, the photon energy which would have been manifested as a characteristic X-ray, is utilized to eject another orbital electron, the Auger electron. This phenomenon is also known as a radiationless transition since the X-rays which would have resulted after internal conversion, are not emitted and another particle is emitted instead.

(2) Gamma Rays:

After the emission (Alpha or Beta Decay) or capture (Orbital Capture, Particle Bombardment, etc.) of a particle, the resulting nucleus is left in an excited state. One way by which the energy of excitation of this nucleus may be decreased is through the emission of gamma rays. The allowed nuclear energy levels are discrete and since gamma rays are the result of transitions by the nucleus from one energy level to another, then gamma ray energies too are discrete; and conversely. The energy of a gamma

photon then is the difference between the excitation energies of the nuclear energy states involved in the transition which results in this particular photon. Gamma emission alone, does not change the proton-neutron composition of the nucleus but may bring the isotope to its ground state (one of lowest energy) through a number of such transition steps; each transition giving rise to a gamma photon emission. The energies of the gamma rays then are indicative of the energy states which the nucleus occupied in its transit to the ground state.

Like X-rays, gamma rays are electromagnetic radiations, as shown by some well-known experiments (e.g., crystal diffraction experiments). X-rays, as previously explained, involve only the extranuclear transitions; while gamma rays on the other hand, are the result of nuclear transitions from one energy state to another as the nucleus proceeds to stability.

There are instances, however, in which the nucleus undergoes a transition to a state of lower excitation energy without the emission of a gamma photon. Instead of emitting the photon, the electromagnetic field of the nucleus interacts with the extranuclear orbits and thereby causes the ejection of one of these electrons. In this case, the energy which would have been emitted in the form of a gamma photon is utilized in the ejection of an orbital electron. The kinetic energy of the ejected electron then is the nuclear transition energy less the energy which bound the electron to its former orbit. These energetic electrons which are emitted from the atom through this process are called internal conversion electrons. Knowledge of the energies of these IC electrons and the orbital binding energies then will give the total energy of this transition.

INTERACTION OF GAMMA RADIATION WITH MATTER

As previously introduced, the Scintillation Technique is based on the interaction of nuclear radiations with phosphors, a special class of substances which emit light upon absorption of these radiations. At this point, it is important to classify the interactions into basic types, with the understanding that the total absorption of the gamma ray energy may (as in actual cases) involve combinations of a number of these basic interactions:

(1) The Photoelectric Effect:

This is the type of interaction in which the total energy of the gamma ray is utilized in ejecting an orbital electron. The resulting energetic electron is called the photoelectron. A free (unbound) electron cannot absorb the gamma energy and become a photoelectron; another body, the nucleus, is necessary for the conservation of momentum in the process. This requirement (bound electron) added to the fact that gamma energies are discrete, explains the discrete nature of photoelectron energies. The kinetic energy of the photoelectron is the difference between the incident-gamma energy and the binding energy of this electron before the ejection.

(2) The Compton Effect:

It is quite possible for an electron to be ejected from the atom even if the energy of the incident gamma ray is not totally utilized in the process. In this type of

interaction, called the Compton Effect, the gamma ray undergoes a scattering process with an electron (considered free and stationary) of an atom, analogous to a two-particle collision (this was predicted by the wave-particle duality of light, or conversely for all electromagnetic radiations in general). This process results with an ejected electron, the Compton electron, and a scattered gamma ray. The resulting wavelength of the gamma ray will be longer due to its loss of energy to the Compton electron. The energy of the Compton electron and the wavelength of the scattered gamma ray may be calculated through the application of the De Broglie Principle and the Conservation Laws of Particle Collisions (relativistic).

It is worthwhile to mention at this juncture that since only a partial transfer of gamma ray energy is involved, the Compton electron carries less kinetic energy than the photoelectron; for incident gamma rays of the same energy.

(3) Pair Production:

In the presence of matter, a gamma ray of energy greater than about 1.02 Mev. (the rest energy of two electrons) may be totally converted into a positive (positron) and a negative (negatron) electron. These particles created from electromagnetic radiation may lose their kinetic energies (each about half the difference between the incident gamma energy and 1.02 Mev.) through ionization by impact on the neighboring atoms, or through their interaction (Coublomb type) with the electromagnetic fields of a nucleus or some orbital-electron distribution. A positron which had been stopped in this manner will then combine with a neighboring electron (free and stationary) to pro-

duce two oppositely-directed gamma photons of 0.511 Mev. each. This process, in which particles disintegrate and radiant energy appears in their stead, is called annihilation; as contrasted to the creation of an electron pair (pair production) from a gamma photon. The annihilation gamma photons may further be converted to particle energies by means of one of the basic interaction (or combinations thereof) already explained.

THE SCINTILLATION SPECTROMETER

From the early scintillation method of counting alpha particle emissions from radioactive substances, has developed a more complicated but more reliable and useful technique. The older method was very inconvenient since visual counting of the number of fluorescences (scintillations) on the Zinc Sulfide target was the only means of getting the disintegration rate. Thus, only weak activities could be investigated.

Recently, the field of nuclear decay studies had been greatly expanded due to important developments in electronic counters and in phosphors. These developments served to give rise to a kind of spectrometric set-up in popular use today.

It is necessary, at this point, to devote a discussion to the Single-Channel Analyzer, the basis of multi-channel Analyzers.

The Single-Channel Analyzer:

This prototype of the multi-channel Analyzer used in the experiment, is made up of a scintillator-photomultiplier assembly (the detector) and some analyzing components (viz., a preamplifier, a linear amplifier, a discriminator and a scaler). A block diagram of this arrangement may be found in Fig. 2.

(1) The Scintillator-Photomultiplier Assembly:

A number of substances have been found to emit

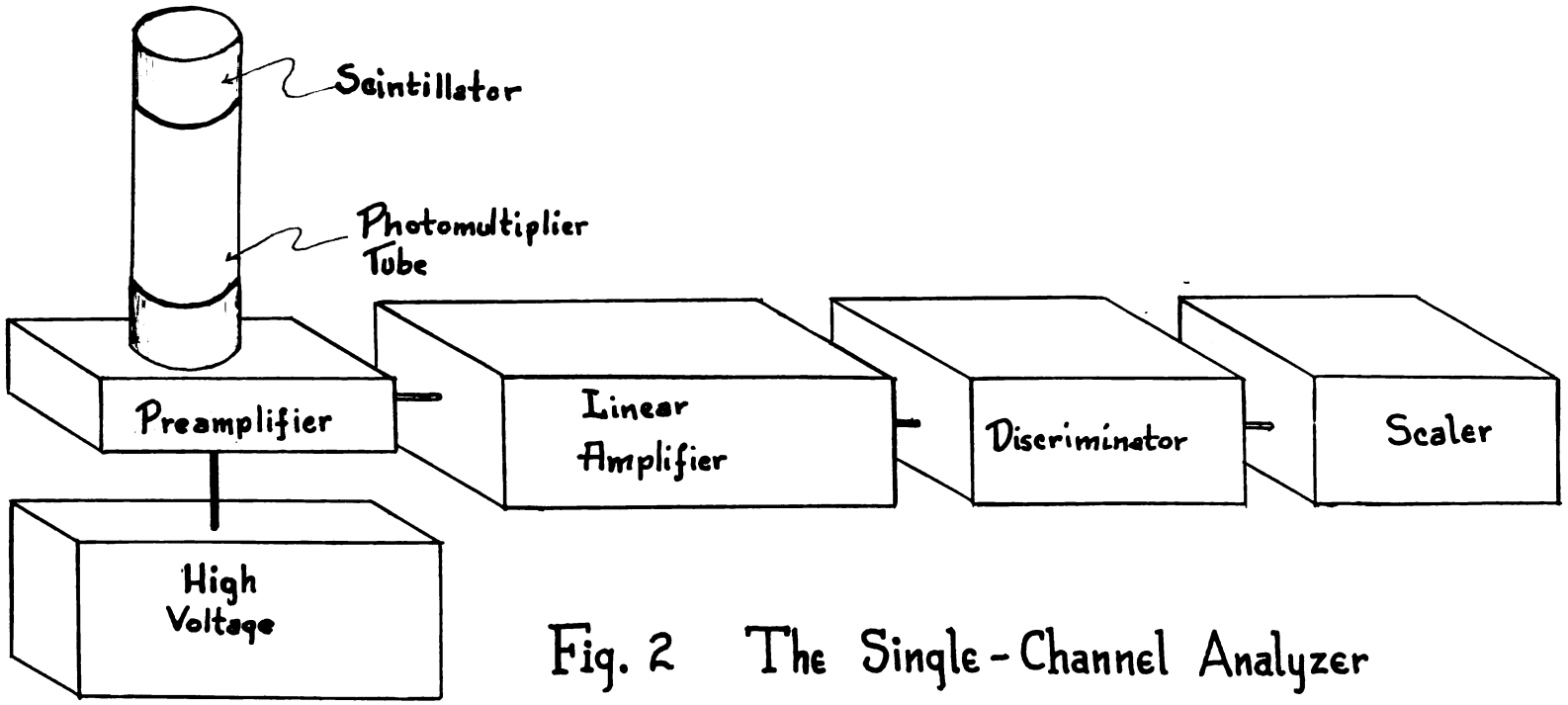

Fig. 2 The Single-Channel Analyzer

light upon absorption of nuclear radiations. These substances are called "phosphors"; their means of absorption of nuclear radiations had been explained in the previous sections.

Gamma radiation energies that are converted to particle energies (i.e., photoelectrons, Compton electrons or electron pairs) are further converted to fluorescent radiation in the phosphor since these particles are easily stopped and their kinetic energies absorbed by the phosphor. On the other hand, gamma rays and X-rays emitted (produced through the annihilation or the photoelectric and Compton processes) near the phosphor surface, may pass through the phosphor without being absorbed and converted to fluorescent radiation. This problem of photon-escape may be remedied to a large extent, by the use of a larger-sized phosphor and the provision for normal incidence of the radiations on the phosphor surface, to improve the possibility of absorption.

Another of a number of requirements for the Scintillation Technique is that as much of the fluorescence (produced by the phosphor) as possible, should be received by the detector, the Photomultiplier tube. The light that is emitted by the phosphor is randomly-directed and must be conveyed towards the receiving end of the photomultiplier tube, the photocathode. This may be accomplished by the use of reflectors which will internally reflect the light to the preferred direction. In addition, the light from other sources than the phosphor must be prevented from finding its way into the photocathode window. This may be solved by masking off the scintillator unto the photocathode window, thus keeping the scintillator-photomultiplier component light-tight from the outside.

The glass encasing the photocathode window also presents a problem. The fluorescence coming into the window

may be reflected (and possibly internally reflected) by this glass layer and thus find its way back into the phosphor and thereby be lost through absorption. This light-loss may be minimized by making an optical joint between the glass window and the scintillator. For instance, the Dow Corning Fluid (No. 200), as a joint, will graduate the optical density of the material confronting the light in its passage into the photocathode; thereby diminishing the reflection of light back into the phosphor. In applying this Fluid on the photocathode window, care must be taken so as not to form air bubbles in the layer (these bubbles may themselves cause the reflections we are trying to prevent). These precautionary measures may be fully understood through Fig. 3. Here the Tl-activated NaI crystal (in the form of a right-circular cylinder 1½ inches in diameter and 1½ inches thick) is encased in an aluminum can (about 0.01 inch thick and with a glass bottom) lined with MgO (reflector); this type of scintillator is available commercially (Harshaw).

The light emitted by the phosphor eventually finds its way to the photocathode, after a series of internal reflections by the scintillator lining. Through the photoelectric process, this light ejects electrons from this photosensitive plate (photosensitivity, in a mild sense, is a measure of the photoelectric response as a function of the luminance). These photoelectrons are then accelerated to a nearby plate, the dynode, by a higher electric potential. The photoelectrons hit the surface of the dynode with such a velocity as to cause the ejection of several electrons, called secondary electrons. The secondary electrons are further attracted to another dynode and their impact gives rise to more secondary emission. These secondary electrons are attracted in a similar manner, by

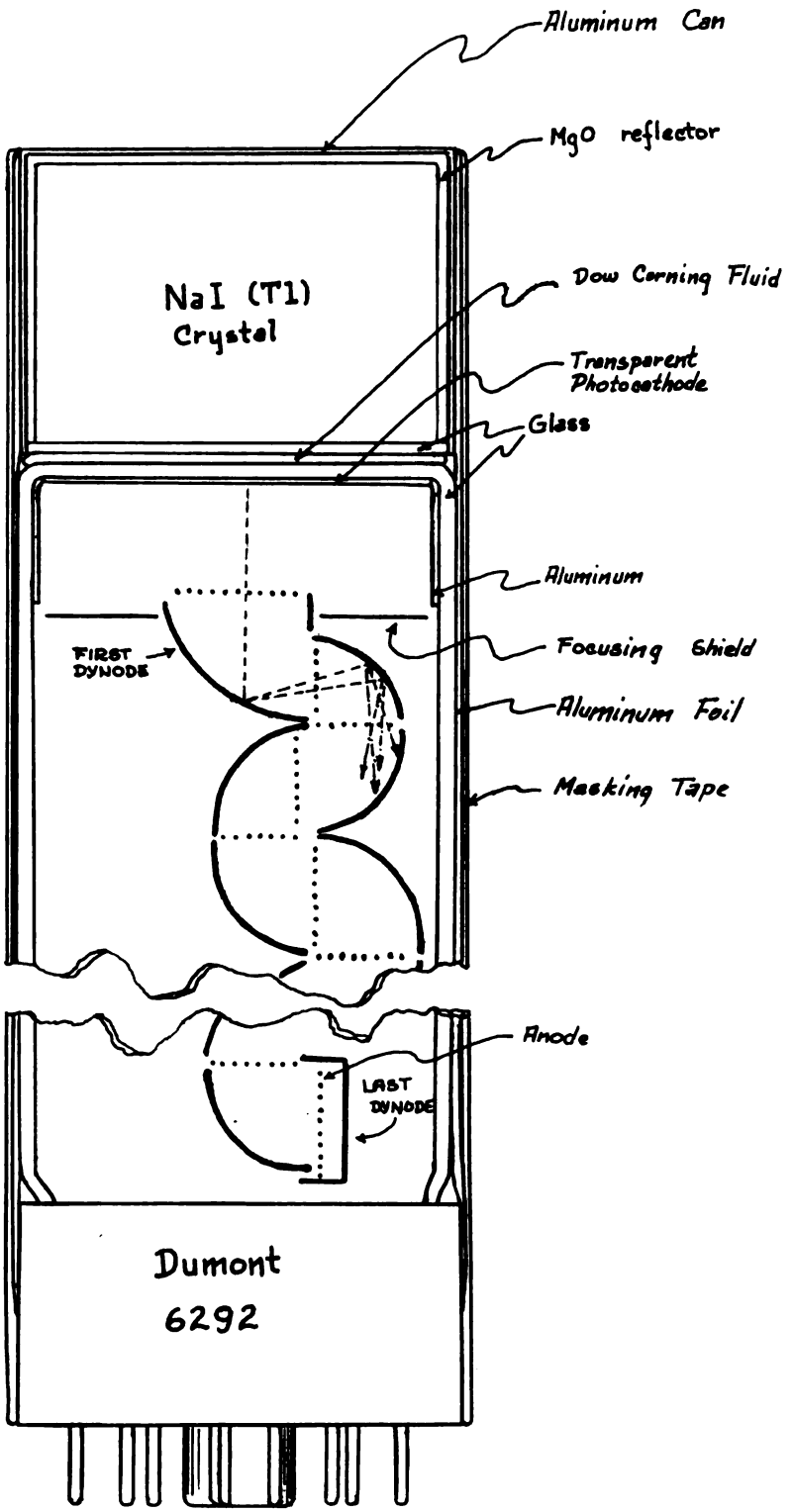

FIG. 3 THE SCINTILLATOR—PHOTOMULTIPLIER ASSEMBLY.

a number of consecutive dynodes which are higher in potential than the preceding ones. The net effect of this repetitive process then, is a progression of the number of secondary emissions; and the number of secondary electrons received by the last plate of the photomultiplier tube, the anode, can be made very large. Some photomultiplier tubes can transfer as much as 10^6 secondary electrons (or even more) to the anode, for every single photoelectron ejected from the photocathode. Thus, a single photoelectron at the start of this progression will register a voltage pulse in the plates of a condenser connected to the anode. In this sense, the photomultiplier component provides pulses which are sufficient in magnitude to be utilized and analyzed by the subsequent electronic components.

It is very important to note at this point, that in the scintillator-photomultiplier pairing, the entire spectrum of the phosphor fluorescent emissions must be within the photosensitivity range of the photocathode.

We have so far, explained what is considered the detector components of the Analyzer; the following sections will be devoted to a description of the analyzing components:

(2) The Preamplifier:

The preamplifier of the photomultiplier serves to amplify the voltage pulses obtained directly from the photomultiplier tube. This is a linear amplifier; the choice of this type of amplification is to preserve the linearity of fluorescence response of the NaI (crystal) phosphor, for instance. Provisions are also made so as to present a low-impedance output to the other portions of the Analyzer, through the use of a Cathode-Follower type (Fig. 4).

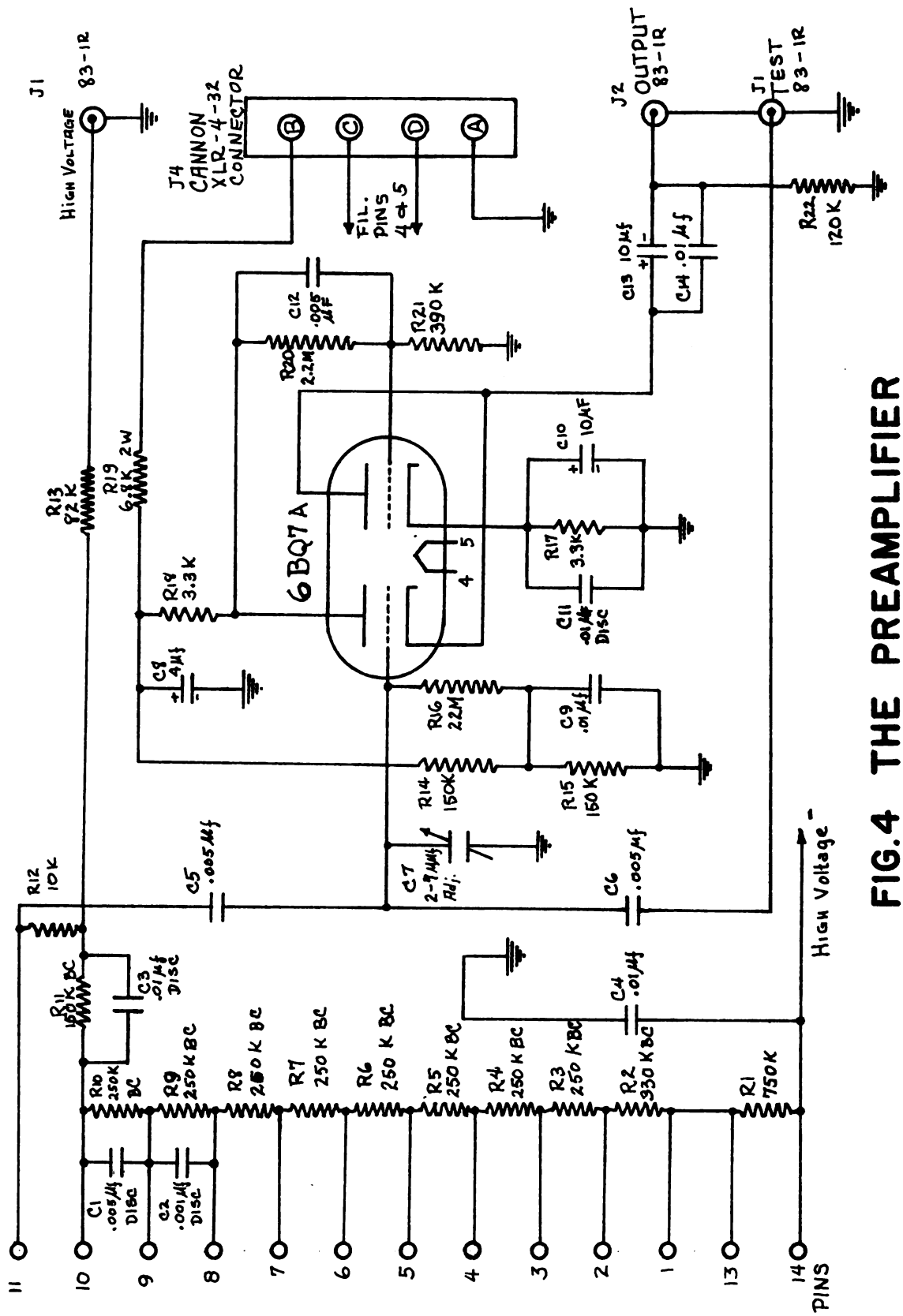

FIG.4 THE PREAMPLIFIER

(3) The Linear Amplifier:

The use of this type of amplification results in output signals of much larger magnitudes and which are in direct proportion to the input. This then provides the convenience of plotting the pulse-height range in a linear scale.

(4) The Discriminator:

In most conventional single-channel analysis, one essentially plots the number of counts for every pre-selected pulse-height interval (into which the entire pulse-height range of the spectrum had been divided). In Elementary Calculus, the entire domain (of independent variables) is first broken up into small intervals and then the height of each of these intervals (the ordinate value) is obtained by integration of the single-valued function under consideration (in each designated interval). Thus, the function is mapped within the desired range. Of course, better approximation is obtained by using smaller intervals.

In single-channel analysis, the number of counts for a pre-selected pulse-height interval (all pulses between the pulse-height E and $E + \Delta E$) must be obtained in order to plot the pulse-height spectrum, by a similar procedure as in the above analogy. The function of the discriminator is to produce an output pulse only when the input pulse-height is within a designated pulse-height interval. That is to say, the discriminator must provide for the setting of the minimum pulse-height value (the Baseline) and the pulse-height interval (the Channel-Width). After the Channel-width had been selected, the number of counts (the value of the "emission" function, refering to the analogy)

for a given Baseline setting is obtained and in this manner, the entire spectral range is swept by the Baseline. The resulting pulse-height spectrum is then the mapping of the number of counts as a function of the pulse-height.

(5) The Scaler:

In the Analysis, the Scaler performs the process of addition (more precisely, it gives a cumulative record of the counts as they take place) and gives the total number of counts for a given pulse-height interval. At the end of the desired time interval, the Scaler displays the total number of counts for the setting. This component is provided with a Start and a Stop switch in order to allow the same time interval for counting in each discriminator setting.

The 256-Channel Analyzer:

In this particular investigation, a modified RIDL 256-Channel Analyzer (Model 3301) was used in conjunction with the type of detector discussed in the previous paragraphs (Fig. 3). The phosphor used was a 1½" X 1½" NaI (Tl-activated) crystal paired with a Dumont No. 6292 photomultiplier tube. The circuit diagram of the preamplifier (Cascade Cathode-Follower Type) involved is shown in Fig. 4.

As the name indicates, the Analyzer effectively combines two hundred and fifty-six single-channel analyzers into a single component. The RIDL Analyzer is equipped with a memory storage, a linear Cathode Ray Display Tube

and a Scaler; aside from its built-in amplifier-discriminator component. The Analyzer may be fed through the Amplifier Input.

The memory-storage component, as the name implies, stores each channel's counts (the channel capacity is 65, 535 counts) and releases them upon demand (PRINT button). There are provisions for memory erasures (MEMORY CLEAR buttons). The Cathode Ray Tube can be used for graphic display of all the two-hundred and fifty-six channel contents (DISPLAY button) simultaneously. The Scaler reproduces the counts of each channel as stored in the memory bank. For convenience, the Analyzer is also equipped with an automatic timer which starts at the beginning of the counting process (COUNT button) and automatically stops the Analyzer at the end of the designated time interval.

A Hewlett-Packard Digital Recorder (Model 560A) was used to obtain a printed record of the actual counts in each channel as stored in the memory bank of the Analyzer. Since the memory capacity for each channel is 65, 535 counts, thereafter the particular channel which over-flowed will immediately start counting from nil; the printed results then turn out accordingly.

The block diagram of the experimental set-up is found in Fig. 5.

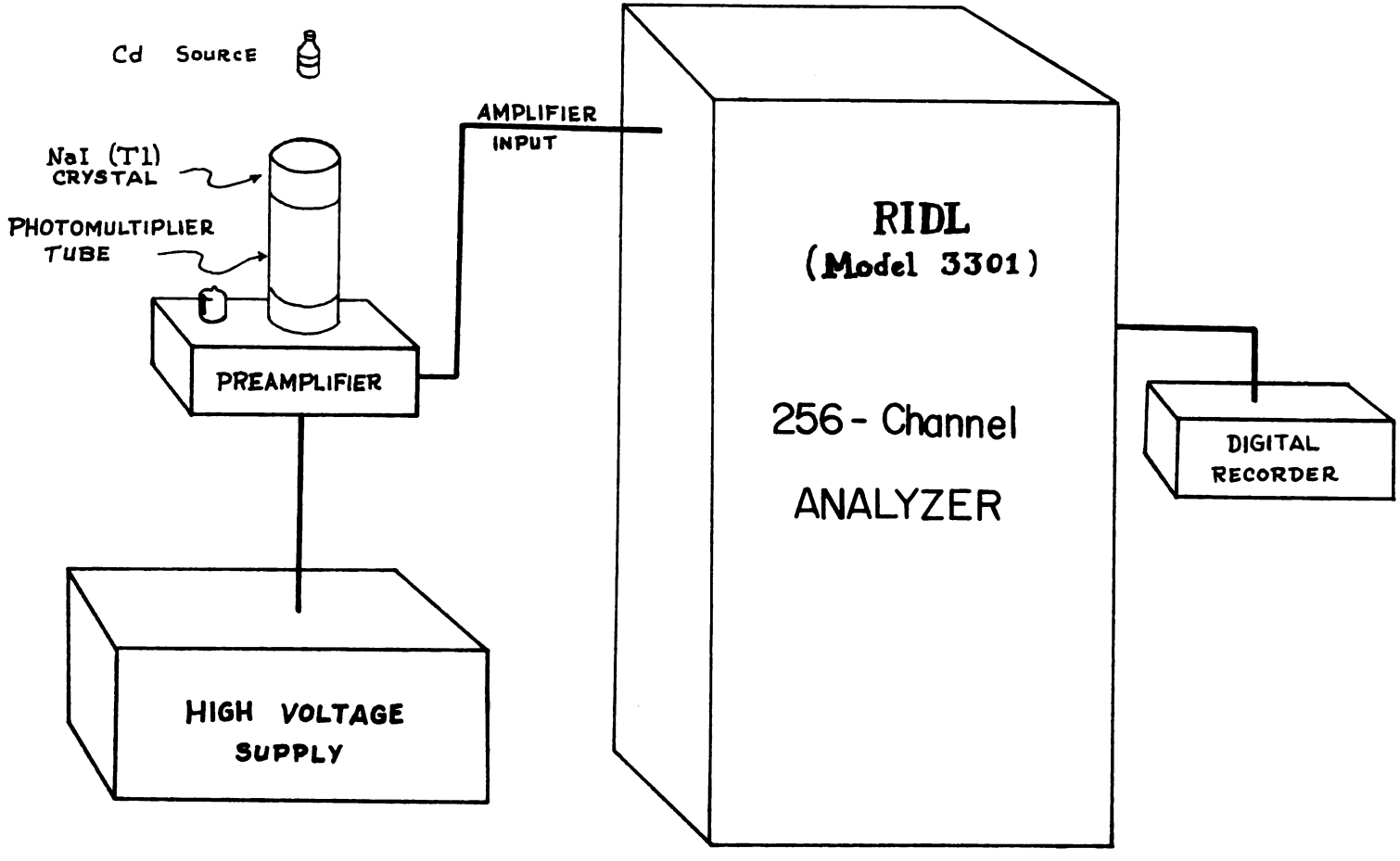

FIG.5 THE ANALYZER ARRANGEMENT.

THE OBSERVED SPECTRA

This portion of the presentation will be devoted to a description of the typical scintillation spectrum obtained with the use of the 256-Channel Analyzer; in particular, that of a single-gamma (i.e., monochromatic gammas) emitter. It must be understood that the spectrum of an isotope emitting gammas of different energies will simply be a superposition of this basic spectrum.

The various interactions of gamma rays with the phosphor resulting in discrete particle or radiation energies (i.e., photoelectrons, Auger electrons, X-rays and annihilation gammas) when absorbed and converted to fluorescence, turn out as pulse-height distributions in the scintillation spectrum. This is because the scintillation, as well as the photomultiplication processes are statistical in nature. Hence, instead of having sharp lines at these energies, Gaussian-like distributions are observed at each of these energy sites. The positions of these peaks then are indicative of the associated energies of these events.

The advantage derived from the use of phosphors which provide pulse-heights per Mev. which are very nearly independent of the energy (e.g., Tl-activated NaI crystal) is that any combination of events in which the gamma energy is totally absorbed in the phosphor produces the same pulse-heights. For instance, a photoelectric event in an iodine atom (this element contributes most, since the process has a high coefficient the higher the atomic number; the concentration of Tl is such that the photoelectric contribution from this element may be considered insignificant) followed by the substantially simultaneous absorption of iodine X-rays, produces the same pulse-height as that due to the total absorption of another gamma of the

same energy through substantially simultaneous events (e.g., Compton events, followed by a photoelectric absorption and the absorption of the associated X-rays). These pulses result in a distribution at the maximum energy. The full-energy peak (as this distribution is most accurately referred to) may be attributed to the most-probable photoelectric process (hence, also called the "photopeak") but in general, it may be attributed to any combination of events which result in total absorption of the gamma energy.

On the high-energy side, this distribution degrades to nil since no possible combination of events (beyond the limits of simultaneity) will produce greater pulse-heights than those from the total absorption of the gamma energy. On the low-energy side, however, the distribution degrades to non-zero counts due to the contributions from pure Compton events. It is quite possible to observe contributions (even another pulse-height distribution, an escape peak) in this region since the associated X-rays have a possibility of escaping from the phosphor when the photoelectric events associated with low-energy gammas (low penetrability) take place near the phosphor surface. In this event, the photoelectric distribution will be below (by an amount equal to the energy of the escaped X-ray photon) the full-energy peak.

The nature of the Compton process itself, leads one to expect a pulse-height distribution at the lower energy range, considering the wide distribution of energies of the Compton electrons. This distribution exhibits a sharp drop or "edge" at the high energy side; this represents the maximum energy that the gamma ray can impart to the Compton electrons. The Compton edge is more pronounced in the spectrum of high-energy gammas since the cross section for the process decreases more slowly with increasing ener-

gy than the cross section for the photoelectric process, and the escape probability for the scattered photons is larger.

The Compton process could take place outside the scintillator; the resulting gammas being scattered into the phosphor. In this event, another pulse distribution, the back-scattered peak, may be superimposed on the Compton distribution. Likewise, the photons scattered by the phosphor may be back-scattered by the materials outside the scintillator (mainly by the glass layers between the phosphor and the photocathode).

Events which result in discrete electromagnetic energies (annihilation gammas) may produce subsidiary pulse distributions when only the associated electron energies (the kinetic energies of the electron pairs) are absorbed and converted to fluorescence by the phosphor. If both annihilation gammas escape the phosphor (i:e., when the pair is produced near the surface of the phosphor), the pair kinetic energies will appear as a pulse distribution 1.02 Mev. below the full energy peak. If only one annihilation gamma escapes, the electron pair energy distribution will be 0.511 Mev. below the full-energy site.

Bremmstrahlung events (emission of inhomogeneous gammas as a result of the changing dipole moment of the atom when the electronic charge is suddenly shifted from the nucleus to a region outside, by the emission of a beta particle) may be manifested as a negative pulse-height distribution, with the maxima at the low-energy limit of the spectrum. This type of distribution is similar to that resulting from amplifier noise (low-energy pulses put out by the amplifier itself), but may be distinguished from the former by analyzing without any radioactive source. This procedure may also be used to investigate extraneous effects on the spectrum (viz., radiations from other

sources nearby, cosmic rays, etc.).

Sample spectra exhibiting some of these characteristics are shown in Figs. 6, 7 and 8.

THE SEARCH FOR THE GAMMA RAY

This particular investigation was prompted by the incompleteness of the data summarized in the Nuclear Data sheets. It was observed that in the proposed decay scheme for Cadmium^{115m} (Fig. 9), there was no definitely established transition which leads to the population of the 1.14 Mev. energy level of the isotope, although a gamma transition from that state to the ground state had been incorporated in the said scheme.

The latest investigation of the decay is summarized in an article by O. E. Johnson and W. G. Smith* wherein the 1.14 Mev. gamma ray was first announced. The experiment was accomplished with the aid of a 256-channel analyzer in conjunction with a 3" x 3" NaI (Tl) crystal scintillator. A full-energy peak was observed at 1.14 ($\pm$ 0.017) Mev., among other gammas. The relative intensity of this gamma did not change after cadmium chemical separation and for over a period of 1.5 half-lives. No further investigation was made on the origin of the 1.14 Mev. energy level; but it was hypothesized that this level may be populated by either a beta or a gamma transition from any of the two over-lying energy states (the 1.30- or the 1.42-Mev state) of the Cd isotope.

These estimates prompted a more-or-less clear-cut plan to support the proposed decay scheme. To constitute an additional experimental proof of the existence of the reported gamma transition, it was planned to display 1.14-Mev photopeak alone (i.e., to remove the superposition effects on the spectrum produced by the two precariously-near gamma rays of 0.935- and 1.30-Mev.). This was to be done by Spectrum Subtraction, using the gamma rays (of energies close

---

* O. E. Johnson & W. G. Smith, Phys. Rev. 116: 992 (1959).

to those of the interfering gammas of Cd) of available isotopes which have simpler gamma spectra (i.e., emitting only one gamma of the desired energy; the presence of an unneeded gamma is also feasible if the energy separation is wide enough so that the Compton distribution of the desired gamma is not masked off by the extraneous one). These requirements are amply satisfied by the isotopes, Na^{22}, and Sc^{46}

The scintillation spectrum of Cd^{115m} (Fig. 6) obtained with the 1½" x 1½" NaI (Tl) crystal phosphor showed very poor resolution at the 1.14 Mev. site. To remedy this, the spectra of Na^{22} and Sc^{46} were obtained through the same conditions as the Cd analysis, except that the amplifier gain was adjusted such that the 1.28-Mev. photopeak of Na^{22} falls on the same site as the 1.30-Mev. photopeak of Cd^{115m} and the 0.88-Mev. photopeak of Sc^{46} falls on the same site as the 0.935-Mev. photopeak of Cd^{115m} (Figs. 7 and 8). The legitimacy of this procedure lies in the fact that the spectral width (or resolution) varies linearly with the amplifier gain. The linearity of the pulse-heights as a function of the scintillation intensity (this may be taken as the energy of the incident gamma ray) allows the effective conversion of the energy of the gamma rays to the desired one by adjustment of the amplifier gain. The gamma rays of Na^{22} and Sc^{46} then had been effectively converted to the energy of the Cd gammas.

These converted spectra (pulse counts as a function of the analyzer channel) can now be subtracted from the spectrum of Cd^{115m} channel-by-channel and counts for counts.

First, both gammas were subtracted from the Cd spectrum. The result of this procedure was poor (Fig. 9). When the Na^{22} spectrum alone was subtracted from the vicinity of the 1.14 Mev. site, the result was much better (Fig. 10). The reason for this better result may be clarified by a comparison of Figs. 6 and 7. It will be noticed that the

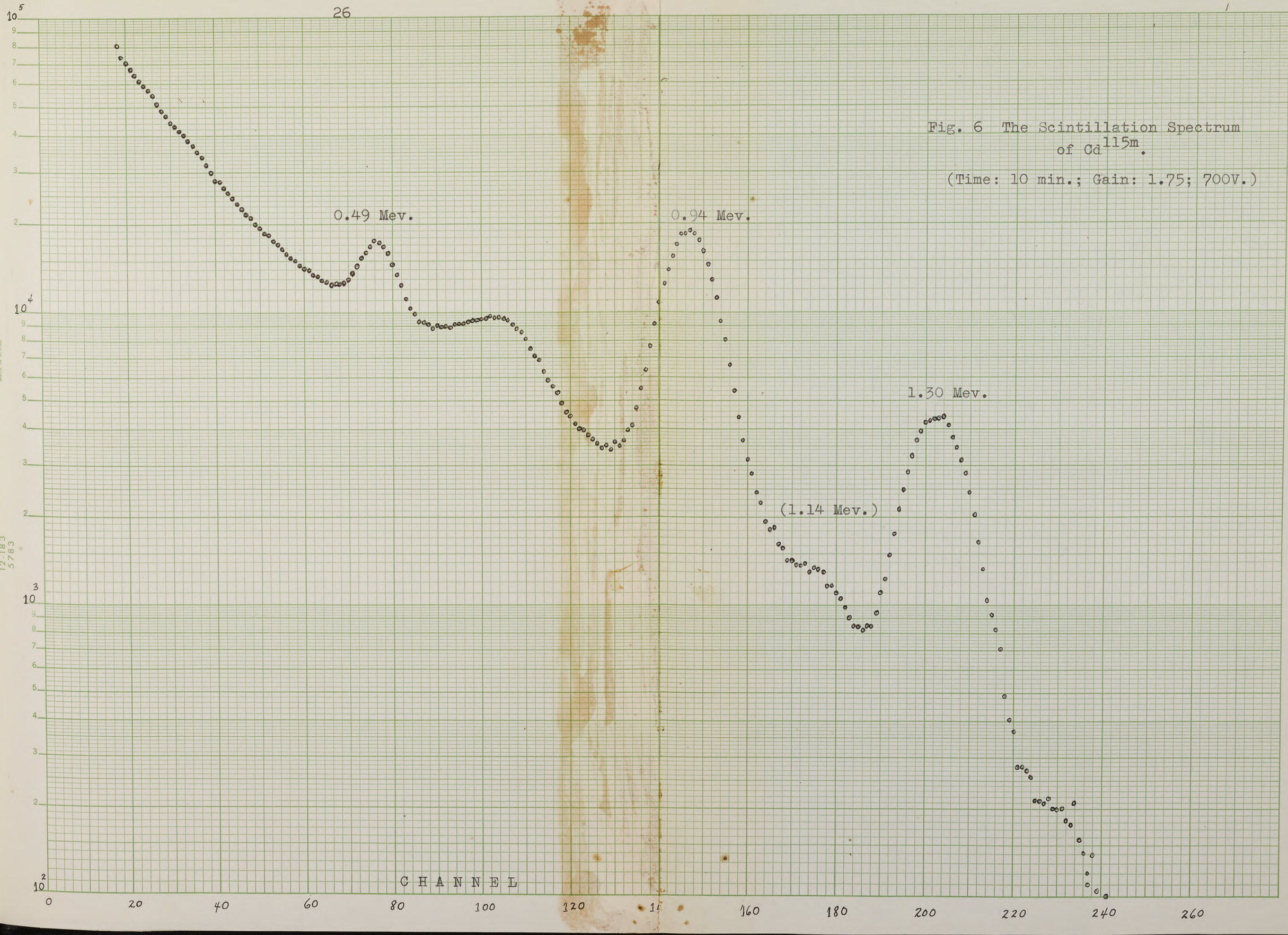

Fig. 6 The Scintillation Spectrum of Cd^{115m}.

(Time: 10 min.; Gain: 1.75; 700V.)

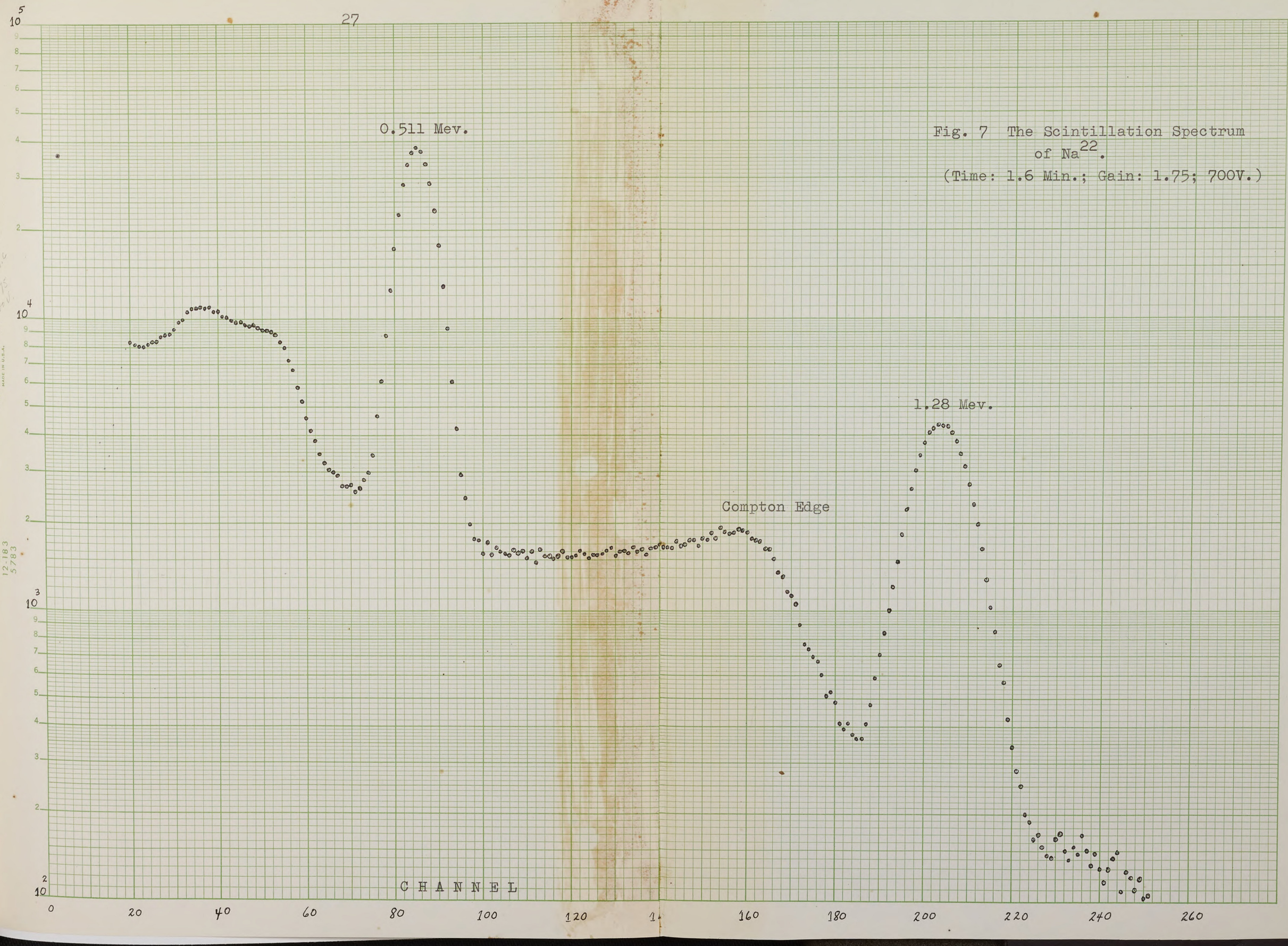

Fig. 7 The Scintillation Spectrum of Na^{22}.
(Time: 1.6 Min.; Gain: 1.75; 700V.)

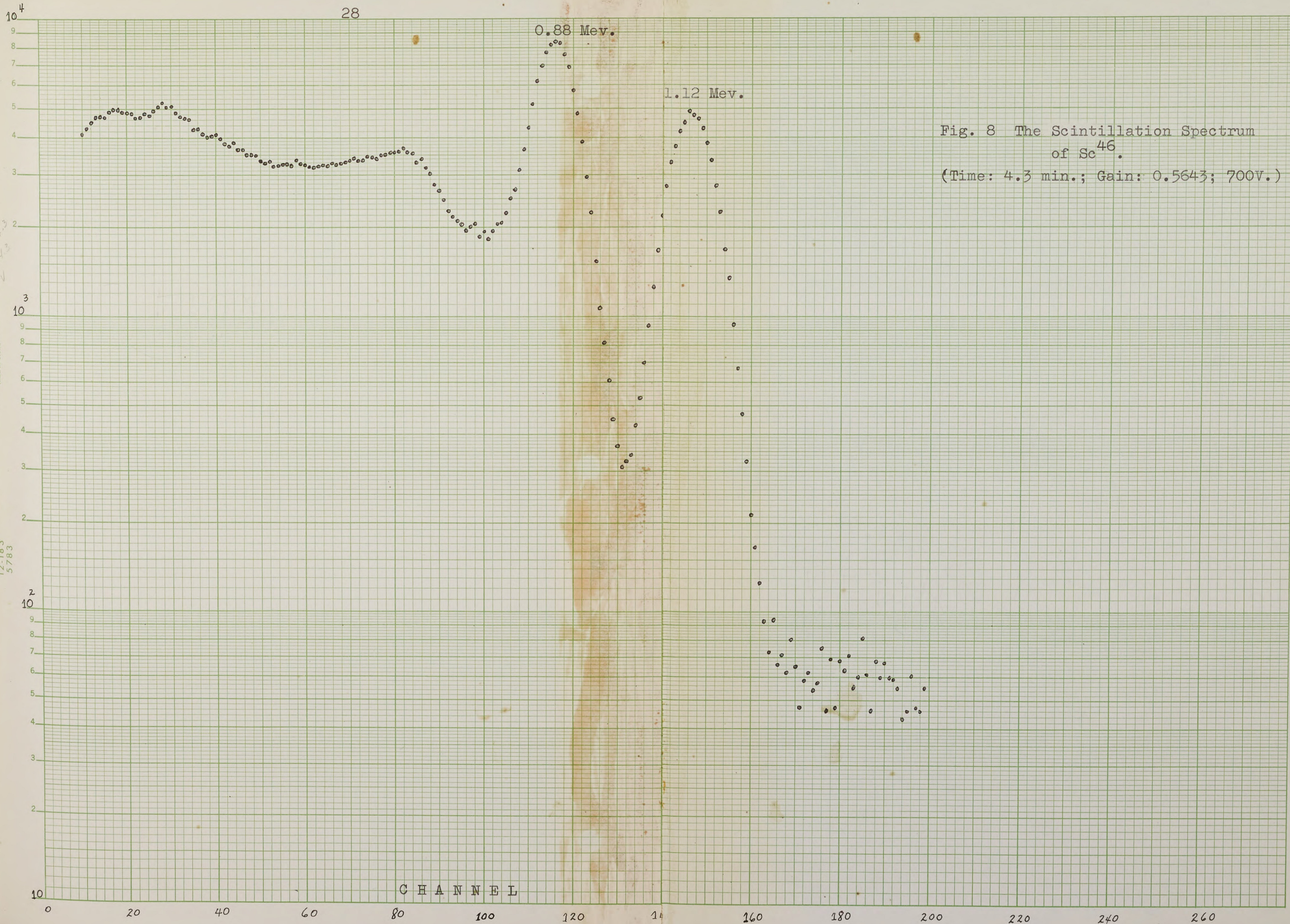

Fig. 8 The Scintillation Spectrum of Sc^{46}.
(Time: 4.3 min.; Gain: 0.5643; 700V.)

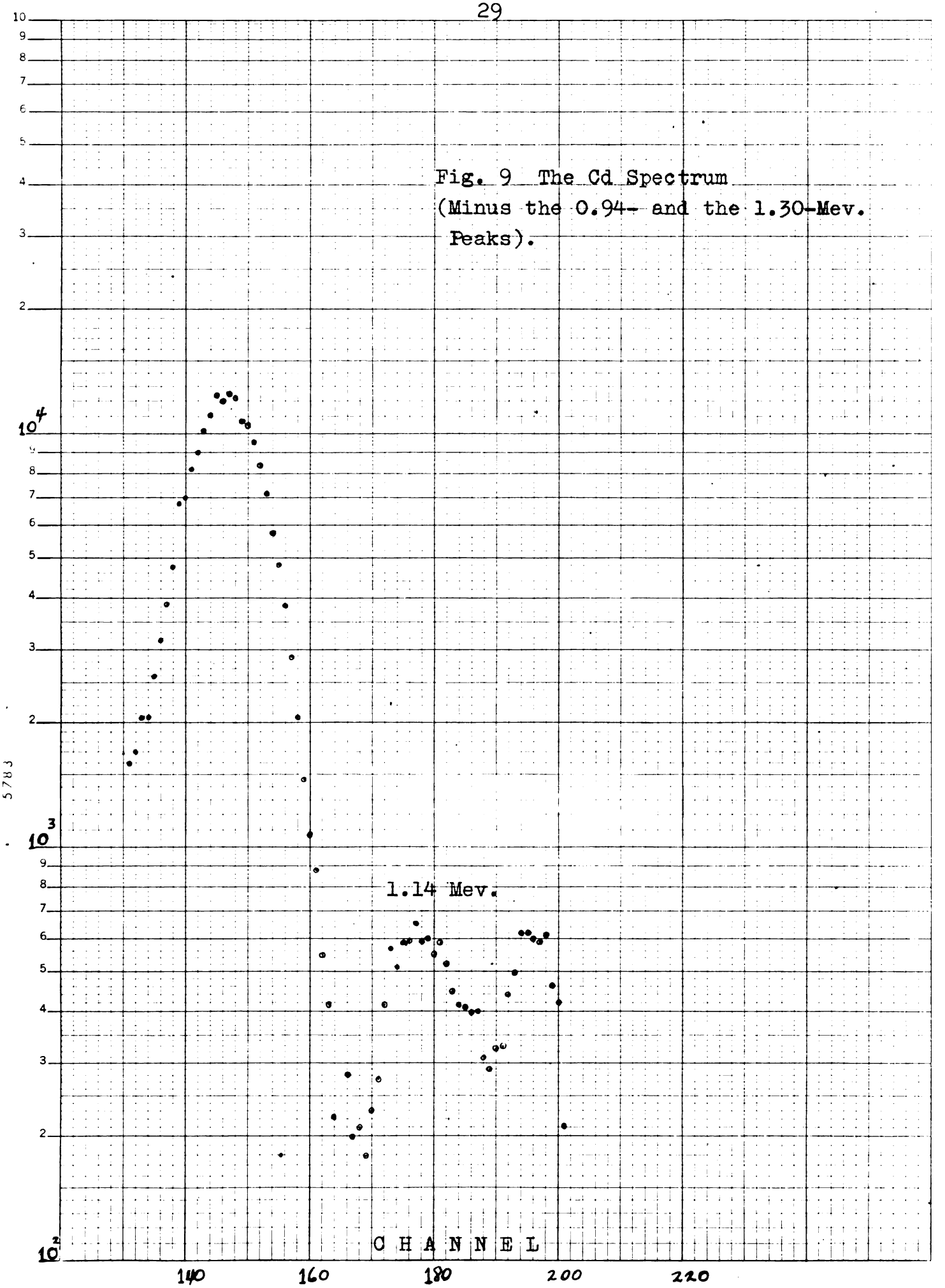

Fig. 9 The Cd Spectrum (Minus the 0.94- and the 1.30-Mev. Peaks).

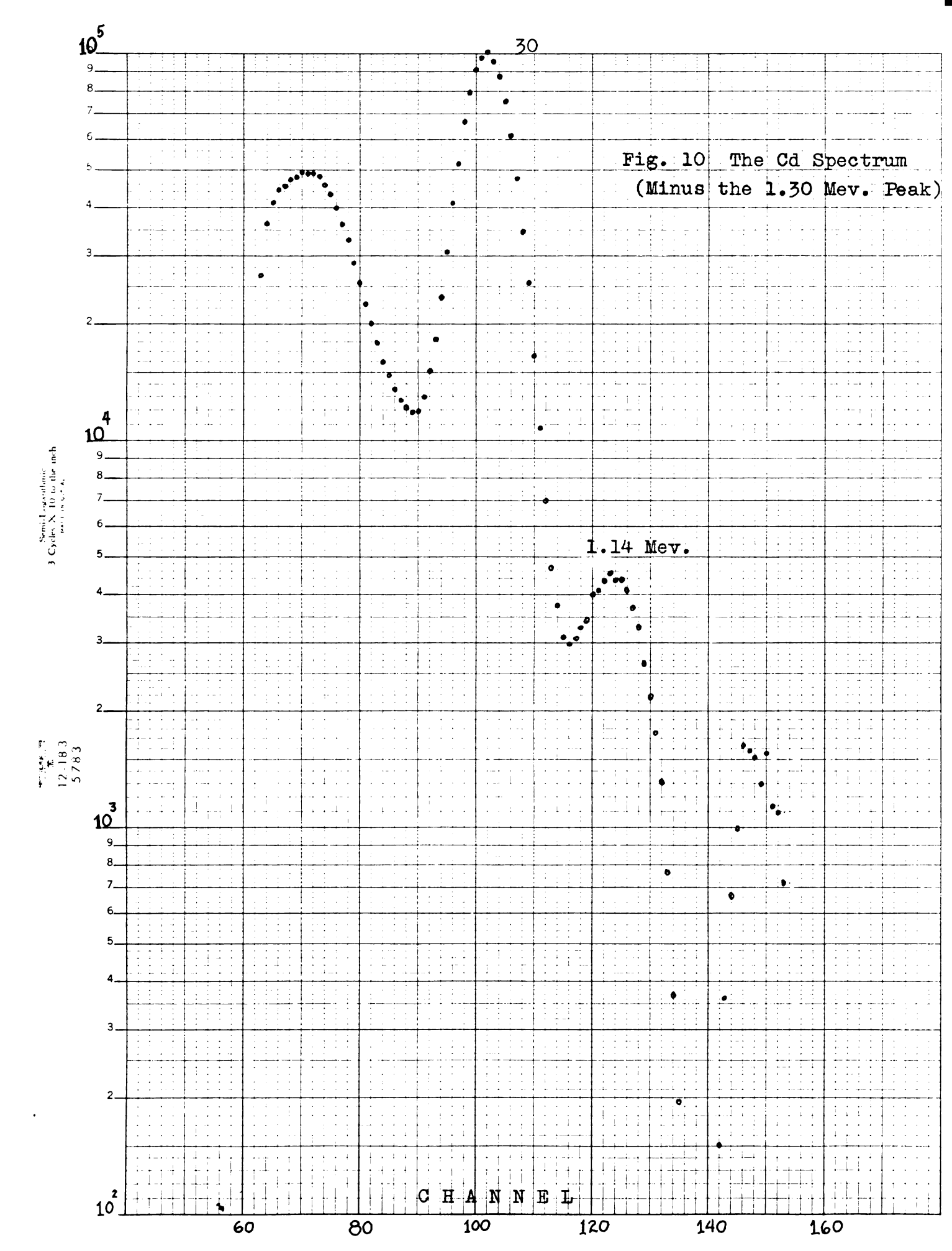

Fig. 10 The Cd Spectrum
(Minus the 1.30 Mev. Peak)

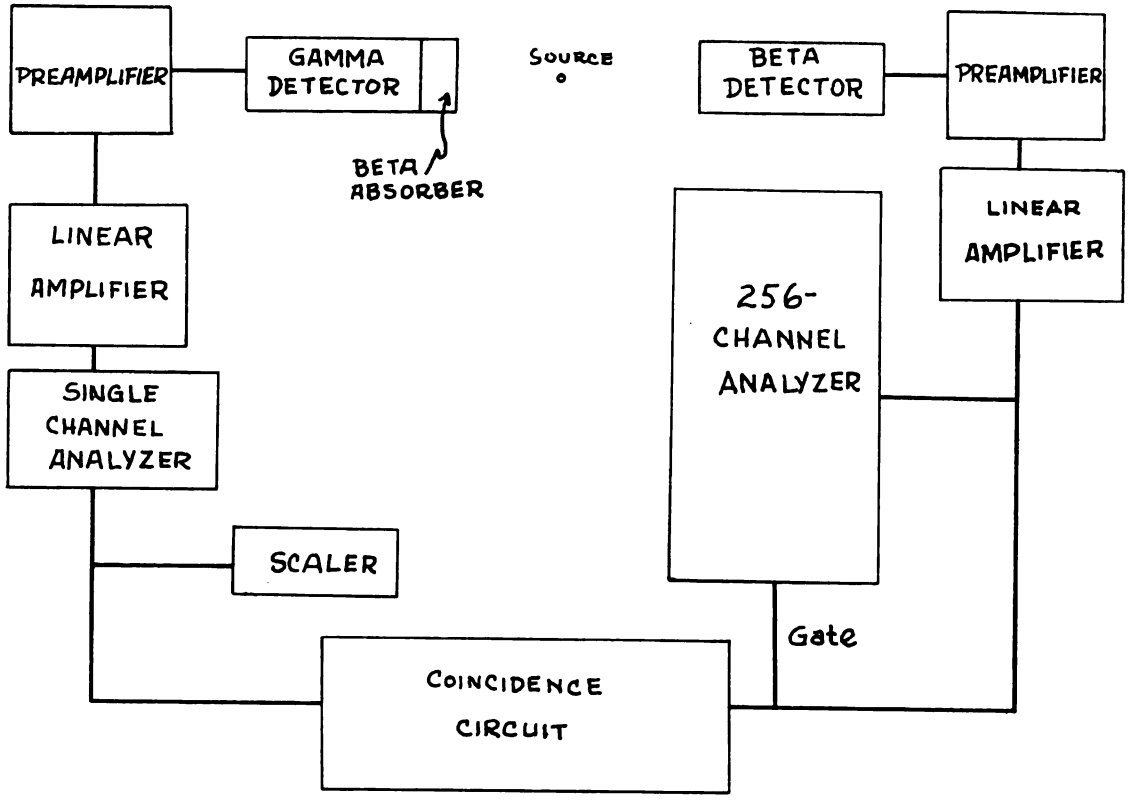

FIG. II THE PROPOSED BETA-GAMMA COINCIDENCE ARRANGEMENT.

Compton peak of the 1.30-Mev. gamma falls at the low-energy slope of the 1.14-Mev. photopeak. The result of this particular step showed a great deal of improvement as compared to that obtained by Johnson et al., using a bigger phosphor. This indicates an importance of the spectrum subtraction in scintillation analysis, especially for very weak intensities (in this case, 0.03%) present in a compound gamma spectrum.

Furthermore, it was observed that the "rise" at the 1.14-Mev. site in both the unsubtracted and in the subtracted spectrum of Cd, grew in the course of the analyses made up to 1.5 half-lives. The improvement can be seen through a comparison of Figs. 9 and 10.

There had been no Cd chemical separation done on the source* and in view of the behavior of this peak as stated above, this gamma is suspected to be emitted by some traces of Zn^{65} (245 days half-life) which may be present in the source. Chemical purification is necessary to ascertain the origin of this weak gamma.

In addition to displaying the 1.14-Mev. photopeak through the spectrum subtraction, a gamma-gamma and a beta-gamma coincidence experiment was also proposed in order to definitely establish the origin of this particular Cd state. A block diagram of the proposed coincidence set-up may be seen in Fig. 11. This experimental arrangement is designed for the beta-gamma portion of the coincidence experiment. For gamma-gamma coincidences, the beta detector need only be replaced by a gamma detector (i.e., adding a beta absorber to the said detector).

However, a closer examination of the Cd decay scheme (Appendix B, Fig. I) revealed a number of difficulties confronting such a coincidence investigation. First, if the 1.14-Mev. state is populated by a beta decay of Cd^{115m},

---

* $Cd(NO_3)_2$ in HNO_3 solution, prepared at Oak Ridge.

then we are faced with the problem of shielding off the 0.485-Mev. gammas (populating the 0.935-Mev. level) from the 0.49-Mev. betas (if any) which is hypothesized to populate the level under investigation. This then requires the use of a high efficiency beta detector (in view of the weak intensity of the betas involved) which is not energized by gammas (of virtually the same energy as the expected betas) which have no relevance to the 1.14-Mev. level. The presence of these extraneous gammas would contribute to the increase of the "chance-coincidence" count rate which in turn, may lead to a doubtful conclusion. Increasing the beta-sensitivity and minimizing the gamma-sensitivity (i.e., using phosphors which are only beta-sensitive) would minimize the "chance" rate, at the detection stage in the analysis. Also, the use of high-efficiency detectors (i.e., larger phosphors) would minimize the error in counting the weak intensities involved.

If the 1.14-Mev. level is populated by gamma transitions from either the 1.42-Mev. level (i.e., a 0.28-Mev. gamma transition) or the 1.30-Mev. level (i.e., a 0.16-Mev. gamma transition), the low-intensity (0.03%) of the related ground state gamma transition would present similar difficulties as in the above possibility. The counts in the low-energy region (below 0.485-Mev.) are extremely high (See Fig. 6), this again would raise the "chance" rate. Another contributory factor to the high count rate in this region is the amplifier noise (these are spurrious voltage pulses put out by the amplifier itself); besides the "background" counts (radiations from other sources).

These difficulties (mainly the unavailability of the vital equipments) gave cause for not pursuing the coincidence investigation any further than evaluation of the problems confronting any future investigation along this same path.

THE LITERATURE RESEARCH

A literature research was undertaken to summarize the latest data on the isotopes: Tc^{96}, Te^{119} and Te^{121}; the findings to serve as a point of embarkation for further investigations of these isotopes. The latest hypotheses as well as some of the informative and novel procedures were included in the summary in order to aid in any future experiments on these isotopes, as well as on any other which may be related.

I. TECHNICIUM^{96}

(1) Source Preparation:

A. Naturally occurring Mo was irradiated with 7-Mev. protons. The sample was then chemically separated from Mo and electrolytically deposited on a foil[1].

B. Tc^{96} alone was produced by irradiation of Nb^{93} foils with alphas of 13.5 and 15 Mev. These energies were chosen to insure mostly (if not totally) an (α,n) reaction on the target.[2]

C. Chemical separation of Tc activities was made by heating the bombarded molybdenum oxide in a glass tube which was open at one end. By temperature control

---

[1] H. Medicus, A Mukerji, P. Preiswerk & G. de Saussure, Phys. Rev. 74: 839 (1948).

[2] H. Easterday & H. Medicus, Phys. Rev. 89: 752 (1953) (2nd Ser.).

the technicium oxide was made to condense in the cooler part of the tube, whereas the less volatile molybdenum oxide was not affected. The activity was then removed with a drop of dilute ammonium hydroxide and mounted on a thin Tygon foil.[3]

(2). Findings of Various Experiments:

A. Gamma-rays:

The 770-, 804-, 840-, 1119- and 312-kev. group was first reported through the discovery of a number of conversion-electron lines using a magnetic lens spectrometer. Furthermore, coincidence experiments showed that the first three of these gammas are emited in a triple cascade (using Bi cathode counters in accord with the measurements in a similar arrangement with Al cathode counters). From the intensity of the 1119-kev. line (estimated from the recoil electrons from brass in the spectrometer) and the coincidence rate, it was concluded that this line is also emitted in the same cascade. The 312-kev. line could only be observed through its converted part. It was also found that the number of cascade transitions is equal to the number of orbital electron captures.[4]

B. Positron Emission:

From a sample prepared by irradiating Nb^{93} with 17-Mev. alphas, a 51.5-minute positron activity was observed using a trochoidal analyzer. Through a comparison of intensities, it was found that there is one positron for every 10^4 transitions to the ground

---

[3] Easterday, et al., loc. cit.

[4] Medicus, et al., loc. cit.

state. Indirect estimation of the maximum positron energy led to a value of approximately 400 kev. This emission constitutes approximately 1% of all beta transitions[5].

C. Conversion-Electron Lines:

The 751-, 786-, 822-kev. lines together with those corresponding to gamma rays of 1119- and 312-kev. were observed by means of a magnetic lens spectrometer. It was also found that 80% of all conversions belong to the first electron group[6].

D. Weak Cross-over Transitions:

The following were reported: 1.65-, 1.89-, and 2.39-Mev. transitions[7].

E. Spin-States and Nature of Transitions:

The data for the 104-hour ground state of Tc^{96}, the absence of strong cross-over transitions in the triple gamma cascade, the absence of positrons as well as a direct transition to the ground state; were the assumptions made in assigning a spin of +7 (at least) to this state. Also, the half-life of 51.5 minutes and a K/L ratio of 1.2 ± 0.3 agree with an assignment of a magnetic 2^3 to the isomeric transition (34.4 kev) and a spin of +4 to the isomeric state. A proton in the $g_{9/2}$ state and a neutron in the $g_{7/2}$ state might add to a spin of 7. For the spin 4, the proton might remain in the $g_{9/2}$ state while the neutron goes over into an $s_{1/2}$ state[8].

---

5 Medicus, et al., loc. cit.
6 Ibid.
7 Preiswerke & Stehelin, Helv. Phys. Acta 24: 301 (1951).
8 Easterday, et al., loc. cit.

F. Proposed Decay Schemes:

(i) From the investigation of conversion lines (From Easterday, et al.; see footnote 2):

Fig. 12 Proposed Decay Scheme of Tc^{96}.

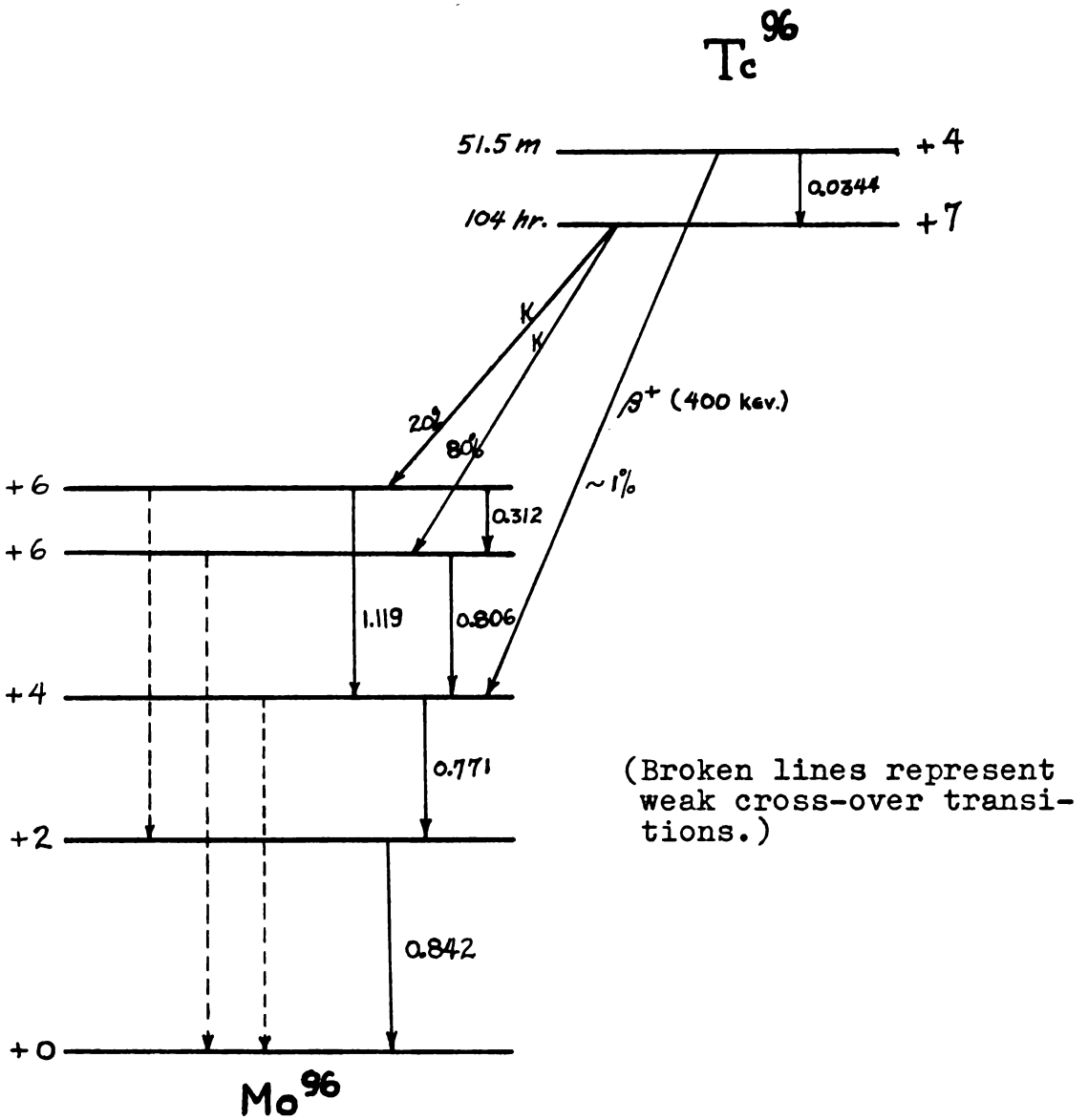

(ii) From spectrometric studies on both Nb^{96} and Tc^{96} (From Preiswerke, et al.; see footnote 7):

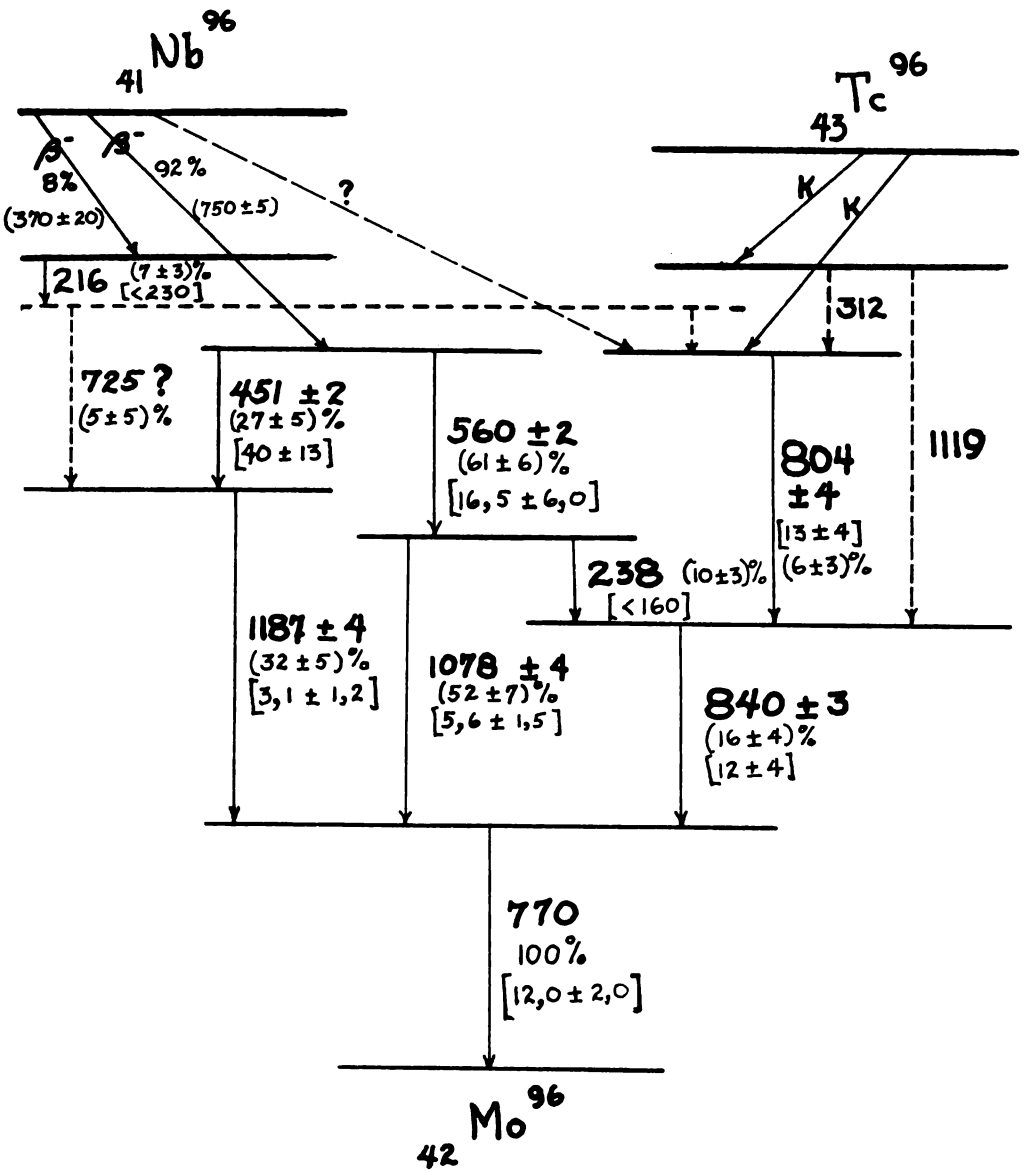

Fig. 13 Proposed Decay Scheme of Tc^{96} and Nb^{96}.

(?)--- Not ascertained.

II. TELLURIUM^{119}

(1) Source Preparation:

A. Metallic Tin was bombarded with 22-Mev. alphas from a cyclotron. A thin layer of the target (1 - 5 mils) was then dissolved in 12N HCl and then Te and Sb carriers were added. The Te metal was then precipitated by adding SO_2 and hydrazine hydrochloride and centrifuged. After decanting and washing, the precipitate was redissolved in dilute HNO_3. Some more Sb carrier was added and the same procedure was repeated. The source was finally obtained by evaporation of the nitrate

Sources derived from the oxides were prepared by fusing with KHF_2, diluting and depositing the Te on a copper plate by the electrochemical process. Then the Te was dissolved and further purified by the SO_2 method. For use with a permanent-field spectrometer, the electrochemical deposit of Te on the thin copper plate can be used directly[9].

B. In another instance, the crosssection was obtained as a function of the bombarding deuteron energy and in this particular investigation, 50-Mev. deuterons resulted in a maximum cross section of 77 millibarns on the 1 mm. thick antimony target [10].

In the spallation study mentioned above, a number of radioactive nuclides have been identified from the result of irradiation of metallic antimony. Chemical separation of Te had been achieved by the follow-

[9] C. Kocher, Allan C. Mitchell, C. Creager & T. Nainan, Phys. Rev. 120: 1348 (1960).

[10] M. Lindner & I. Perlman, Phys. Rev. 78: 499 (1950).

ing process. The irradiated antimony metal was dissolved by covering with concentrated hydrofluoric acid and the dropwise addition of concentrated nitric acid. After dilution, Te carrier was added and the solution made 0.1M in HCl. Yttrium and silver products were precipitated as yttrium fluoride and silver chloride. The remaining solution was then buffered with sodium acetate and the sulfide-insoluble activities were removed by the addition of indium and precipitation of indium sulfide with hydrogen sulfide. After expelling the excess hydrogen sulfide, the supernatant solution was then evaporated to dryness and taken up in 2M HCl. Tellurium was reduced to the elemental state by treatment of the hot solution with sulfur dioxide[11].

(2) Apparatus:

A variety of instrumental set-up were used in one particular investigation of the Te^{119} isotope. To study and measure the positron distribution and the energies and intensities of IC electrons, for instance, a magnetic lens spectrometer was used. To measure the lower-energy IC electrons, a permanent field photographic recording magnetic spectrograph was used[12]. In another case, IC electrons of 0.2-Mev. and 0.5-Mev. were measured with a low-resolution beta-ray spectrometer[13].

The gamma-rays and their relative intensities were studied by means of a scintillation spectrometer. The 3" X 3" NaI (Tl) crystal was used in conjunction with a 5-inch (dia.) Dumont Type 6364 photomultiplier tube, and the pulse-height distribution was fed into a

---

11 Lindner, et al., loc. cit.
12 Kocher, et al., op. cit., p. 1349.
13 M. Lindner & I. Perlman, Phys. Rev. 73: 1124 (1948).

100-channel analyzer[14].

The gamma-gamma coincidence investigation was carried out using two 1½" X 1½" NaI (Tl) crystals, while anthracene phosphors were used in the positron-gamma coincidences. Two types of coincidence circuits were used for both cases. A "fast-slow" coincidence circuit with a resolving time of 0.1 μsec. was used with two single-channel analyzer, and also with a 100-channel analyzer having a single-channel analyzer as the selector. The other type of circuit used two RCA 6810-A fourteen-dynode tubes. The anode signal was first put through a limiter, clipped and then fed into a fast coincidence circuit. The pulses which allow energy selection were taken from the seventh dynode, passed through a linear amplifier and single-channel pulse-height analyzer and into a triple coincidence circuit, into which the pulses from the fast coincidence circuit were also fed. To display the coincidence spectrum on the 100-channel analyzer, the analyzer was placed in one leg of the slow coincidence circuit. A single-channel analyzer on the other leg selects the energy of the gamma-ray of interest. The resolving time of this circuit was approximately 15 μsec.[15].

(3) Experimental Findings:

A. Positrons:

(a) Higher-Energy group:

This group showed a half-life of 5.6 days, an end-point energy of 2.7 Mev., and a log ft of 7.90.

[14] Kocher, et al., op. cit., p. 1349.

[15] Ibid.

This log ft value is too high to fit in the systematics of Te^{119}. However, if this positron group is ascribed to the 3.5-min. Sb^{118} which is in equilibrium with its parent Te^{118} as a result of an (α,2n) reaction; its end-point energy and log ft value (5.6) are in reasonable agreement with the previous information on Sb^{118}. Further study was made in order to verify that these high energy positrons come from Sb^{118} as a result of the nuclear reaction on the metallic antimony. Plates 0.001 mm. thick were milled off from the antimony target and the ratio of the number of positrons of the higher energy to those of lower energy were studied as a function of the depth in the target. The ratios decrease very rapidly as a finction of the depth below the surface, indicating that it is by an (α, 2n) reaction.[16]

(b) Lower-Energy Group:

After correcting for the higher energy group, this particular positron group exhibited a half-life of approximately 13 hours (this value is not considered very accurate), and an end-point energy of 0.627 $\pm$ 0.002 Mev..[17]

B. Gamma Rays:

The following table gives the observations from the gamma ray investigations. The results given there were obtained when ordinary metallic tin was alpha-bombarded so that lines owing to other long-lived Te

---

[16] Kocher, et al., op. cit., p. 1350.

[17] Ibid.

activities were present. These served as checks on the energy calibration of the permanent field and the magnetic lens spectrometers. The relative intensities were taken early enough in the run so that the lines arising from long-lived activities made a negligible contribution:[18]

Table I. Energies, relative intensities, and half-lives of the gamma rays of Te^{119}

Energies from IC lines:		Scintillation spectrometer:		
Gamma-ray Energy (kev.)	Half-Life	Gamma-ray Energy (kev.)	Relative Intensity	Half-Life
153.0 ± 0.1	5.3 days	155	112	
270.0 ± 0.1	4.38 ,,	270	54	
. . .	. . .	511 (ann. rad.)	...	
645.0 ± 1	15 ± 2 hr	645	(20)	15 ± 1 hr
. . .	. . .	930	22	
. . .	. . .	1100	21	
1221 ± 1	4.6 days	1220	100	4.8 ± 0.2 d.
. . .	. . .	1760	(1)	18.5 ± 1 hr.
. . .	. . .	2120	7	4.5 ± 0.3 d.

It was observed that the lines can be classified according to their half-lives: the 0.645- and the 1.76-Mev. lines (15-20 hr. half-lives), and the rest (of about 5 days half-life). The experiments showed that there seems to be no growth or decay of one system from the other; implying that the lifetimes of the of the isomeric states involved are governed to a large extent by their several transition probabilities

[18] Kocher, et al., op. cit., p. 1349.

to the states of Sb^{119}, rather than by the gamma-ray lifetime for isomeric transitions in Te^{119}. Similar situations exist in a number of Te isomers.[19]

(a). Results of Coincidence Experiments:

Table II. Coincidences in the 4.7-day Te isomer[20]

Selected Gamma-rays (Mev.)	Gamma-rays in Coincidence
2.12	0.270
1.22	0.930, 0.153
1.10	0.270

There was no coincidence between the 0.645- and the 1.76-Mev. gamma-rays. Positron-gamma coincidence tests produced null results with the 0.645-, the 1.76- or the 0.153-Mev. gamma-rays. With this particular coincidence experiments on the 16-day Te isomer, the extraneous effects of an (α,2n) reaction on the target have been corrected for.[21]

(b). Internal Conversion Coefficient of the 0.645-Mev. transition:

A comparison method was used with the aid of a magnetic lens spectrometer, with Cs^{137} as the standard. IC electrons were counted for both isotopes and the intensities of their respective gamma-rays were then measured with a calibrated scintillation counter. This yielded an IC coefficient $\alpha_{tot} = 4 \times 10^{-3}$

19 Kocher, et al., loc. cit.

20 Ibid.

21 Kocher, et al., op. cit., p. 1351.

(± 10%), on the 0.645-Mev. gamma-ray. The theoretical value for the (K + L) is either 3.9×10^{-3} or 4.9×10^{-3}; the experiments are not good enough to differentiate between α_2 and β_1 but it is quite clear that this particular line cannot have either an E3 or an M3. This particular gamma-ray is of M1 or E2 character so that its state of origin must be of short life compared with the resolving time (10^{-7} sec.) of the positron-gamma coincidence experiments. An assumption of a long-lived state cannot account for the absence of positron-gamma coincidence with this particular line.[22]

(4) Hypotheses:[23]

The product nucleus, ${}_{51}Sb^{119}$ has one proton outside of a closed shell. The ground-state configuration for this nucleus would be 5/2 +, 7/2 +, 3/2 +, and 1/2 + . However, these experiments are not detailed enough to give definite information on these predictions. The reported half-life of the 0.153-Mev. state, 0.84×10^{-9} sec.[24] is in agreement with an M1 (10%) + E2 (90%) mixture for the transition from this state to the ground state. The K/(L + M) ratio of this line was found to be 7.850. The theoretical values are M1 = 8.35 and E2 = 3.48. Such a hypothesized mixture would then agree with a 7/2 + to 5/2 + transition. The K/(L + M) ratio for the 0.270-Mev line has also been measured and found to be 5.77 which when compared with the theoretical values, M1 = 5.32 and E2 = 4.16 (similar mixture as the 0.153-Mev. transition) would

---

[22] Kocher, et al., op. cit., p. 1351.

[23] Kocher, et al., op. cit., p. 1352.

[24] T. D. Nainan, Bull. Am. Phys. Soc. 5: 239 (1960).

agree with a 3/2 + to 5/2 + transition. This implies that the level assignments for the excited states of Sb^{119} may be correct, although a final verification by means of an angular correlation experiment may be necessary since the above ratios are not very sensitive functions of the multipole order in this region.

The ratio of the relative number of IC electrons of the 0.645-Mev. line to the number of positrons of the low-energy group, the figures for the IC coefficients and the relative intensities of the two gamma-rays (from the short-lived isomer); these estimates led to a log ft value of 6.9 for the positron transition and 5.2 for the transition to the 0.645-Mev. state. This implies that the latter transition is a once forbidden.

It was also hypothesized that the $h_{1/2}$ state lies higher than the $s_{1/2}$ state and that the $d_{3/2}$ state lies close to the $h_{1/2}$ state, insuring a transition of long half-life (about 200 days) which cannot compete with the 5-day electron capture. Hence the gamma-ray resulting from this transition would be extremely weak. The weak positron group would be in agreement with a transition to a 3/2 + state but not to a 5/2 + state. A contribution from the weak 16-hour positron activity may account for the somewhat-shorter half-life (4.38 days) of the 0.270-Mev. state as compared to the other states associated with the 5-day decay. The allowed nature (once forbidden) of the 0.645-Mev. state would suggest that this is the 1/2 + state of Sb^{119}. If the assumptions are correct, the $s_{1/2}$ state of Te would lie 1.92 Mev. above the ground state of Sb^{119} and the $h_{11/2}$ state at greater than 2.39 Mev. The $h_{11/2}$ - $s_{1/2}$ energy difference would then be 400 to 500 kev.

(5) Proposed Decay Schemes:

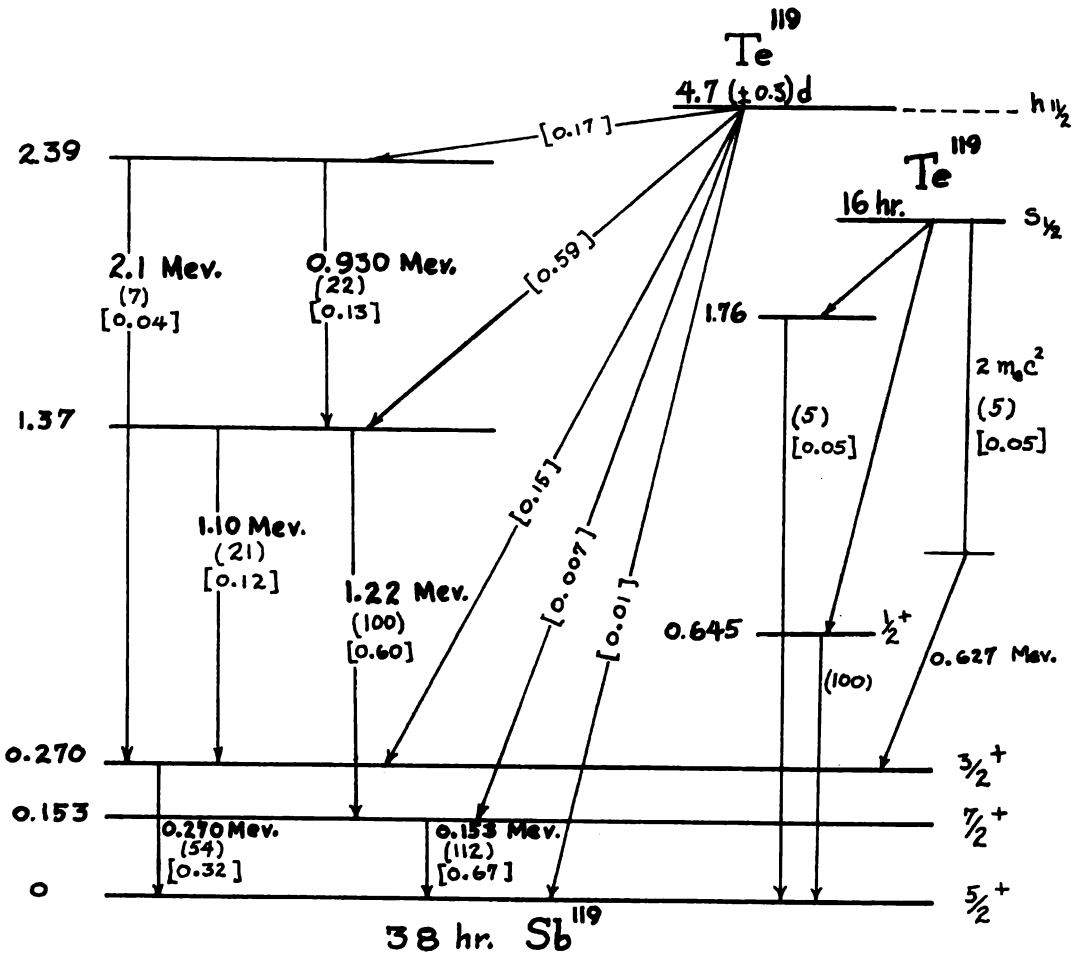

Fig. 14 Tentative decay scheme for Te^{119}. For the 5-day activity the relative intensities of the gamma-rays are given in parentheses, with the intensity of the 1.22-Mev. gamma ray = 100. The fraction per disintegration is given in square brackets.[25]

---

[25] Kocher, et al., op. cit., p. 1352.

III. TELLURIUM^{121}

(1) Source Preparation:

A. Hilger Sb metal lab No. 11707 was activated with 10-Mev. deuterons. This metal was then dissolved in aqua regia and then evaporated to dryness. The residue was taken up by the hot dilute HCl and an excess of tartaric acid. Te was precipitated from this solution by hydrazine dihydrochloride.[26]

B. Naturally-occuring antimony was irradiated with 15-Mev. deuterons from a cyclotron; a (d,2n) reaction produced mixed Te^{121} and Te^{123}. One gram of the irradiated antimony and 1 mg. of Te-free selenium were dissolved in aqua regia, heated to dryness, and then redissolved in 3N HCl. Both the selenium and the radioactive Te were precipitated by bubbling SO_2 through the solution. The selenium acts as a carrier which eliminates the need for adding Te carrier in this step. The precipitate was then dissolved in the smallest possible quantity of 12N HCl (about 5 ml.). One microgram of Te, which had been dissolved in aqua regia, heated to dryness and then redissolved in 12N HCl, was added as a carrier. This minute amount suffices because we have only a very small amount of material at this point, the great bulk of material being removed in the first separation. SO_2 was again bubbled through the solution. Only Se is precipitated with 12N HCl, the Te remaining in the solution. By this method a source of 100 μcuries activity having a mass of 1 μg. was prepared.

[26] J. E. Edwards & M. L. Pool, Phys. Rev. 69: 140 (1946).

The Te was vacuum-evaporated from a small pyrex oven unto a formvar film (<9 μg/cm.^{2}) which had been coated with either aluminum or silver conducting layyers (<4 μg/cm.^{2}). The thickness of the source material itself was less than 1 μg/cm.^{2}.[27]

(2). Results of Various Experiments:

A. The high intensity of the observed Te X-rays is accounted for by K-capture in Te^{121} followed immediately by internal conversion of the 0.214-Mev. gamma-ray in the singly-ionized K-shell. The X-ray is then emitted by the Sb atom having both K-electrons missing. The X-ray wavelength emitted by this process would differ slightly from that of Te.[28]

Furthermore, since both Sb X-rays and a 0.575-Mev. gamma are associated with the 154-day as well as the 17-day Te^{121}; these two activities logically constitute the isomeric pair.[29]

B. Gamma-rays:

(a). 0.070 Mev. (scintillation spectrometer)[30]
(b). 0.082 Mev. (through IC electron-gamma coincidences)[31]
(c). 0.214 Mev (,, ,, ,, ,,)[32]
(d). 0.506 Mev. (scintillation spectrometer)[33]

---

27 N. Goldberg & S. Frankel, Phys. Rev. 100: 1351 (1955).
28 Edwards, et al., loc. cit.
29 Edwards, et al., op. cit., p. 144.
30 Bhatki, Gupta, Jha & Madan, Nuovo Cimento 6: 1466 (1957).
31 R. Katz, R. Hill, & M. Goldhaber, Phys. Rev. 78: 9(1950).
32 Bhatki, et al., loc. cit.
33 Ibid.

(e). 0.575 Mev. (scintillation spectrometer)[34]
(f). 1.130 Mev. (,, ,,)[35]

C. Radiations in Coincidence:

(a). The 0.214-Mev. gamma and electrons from the 82 kev. transition (through a variable field, 180° focusing beta-ray spectrometer with a "double-slit" spectrograph insert).[36]

(b). The 0.506-Mev. and the 0.070-Mev. gammas (scintillation spectrometer).[37]

D. Relative Intensities of Conversion Lines:[38]

Table III.

IC Line (kev.)	Area under line (arbitr. units)	Peak height (arbitrary units)	Relative Intensity (ave. of area & peaks)
82-K	3420 ± 850	306 ± 26	75
82-L	3930 ± 980	473 ± 26	100
82-M	560 ± 140	107 ± 32	18
214-K	371 ± 37	108 ± 7	16
214-L	53 ± 5	14 ± 5	2.2

[34] Bhatki, et al., loc. cit.
[35] Ibid.
[36] Katz, et al., loc. cit.
[37] Bhatki, et al., op. cit., p. 1467.
[38] Katz, et al., op. cit., p. 10.

E. Nature of the Isomeric Transitions:[39]

Using the above relative intensity values, IC coefficients and N_K/N_L ratios were computed and the values so obtained are between a 2^4 (mag.*) and a 2^5 (elec.*) for the 82 kev transition, and between a 2^1 (mag.**) and a 2^2(elec.*) for the 214-kev. transition. Furthermore, the N_K/N_L ratio so obtained for the 214-kev. transition is between a 2^1 (mag.†) and a 2^2 (elec.†). The theoretically obtained half-life $\times (1 + Ne/N\gamma)$ was found to be 1.0×10^{10} sec. for the 82-kev. transition.

F. Angular Correlation Measurements:[40]

Using a thin-lens beta spectrometer as the fixed detector a scintillation counters for the movable detectors, the measured correlation was found to be of the form: $1 + A_2P_2(\cos \Theta)$; in agreement with the theoretically predicted angular correlation for the known spin sequence in the Te isomers (11/2 —— 3/2 —— 1/2). The measured values of A_2 (corrected for geometry) are: -0.015 ± 0.007, -0.007 ± 0.007, and -0.10 ± 0.04 for the K-, L-, and the K-K cascades respectively for Te^{121}. Comparing the first of these coefficients with theory, shows that the second transition is a mixture of $(5.6 \pm 0.50)\%$ E2 and 94.4% M1.

---

39 Katz, et al., op. cit., pp. 10-11

* Theoretical values for this ratio was obtained from Hebb & Nelson (Phys. Rev. 58: 486, 1940) and Drell (Phys. Rev. 75: 132, 1949).

** Theoretical values for this ratio was from the curves by Lowen et al.(Phys. Rev. 75: 529, 1949).

† Theoretical values for this ratio was from Rose, et al., "Tables of K-shell Conversion Coefficients" (privately distributed).

40 Goldberg, et al., op. cit., p. 1350.

Using the Biedenharn and Rose notation, the ratio of reduced matrix elements is plus. The results of the K-K angular correlation is consistent with the K- γ correlations and are used to prove that the correlations, which are smaller than the M4-M1 correlation, cannot result from reduction of the M4-M1 correlation by the action of extra-nuclear fields.

G. Utilizing the data obtained by microwave techniques, the electric quadrupole moment for this daughter nucleus was found to be; $Q = -1.3 \times 10^{-24} cm^2$. [41]

In another investigation, where a hollow-cathode discharge tube was used and a Fabry-Perot etalon for resolving the hfs; the result was, $Q = (-0.53 \pm 0.10) \times 10^{-24}$ cm^2. It was further explained why the original value given above is not valid.[42]

---

[41] G. Sprague & D. Tomboulian, Phys. Rev. 92: 105 (1953).

[42] K. Murakawa, Phys. Rev. 100: 1369 (1955).

H. Proposed Decay Schemes:

(i)

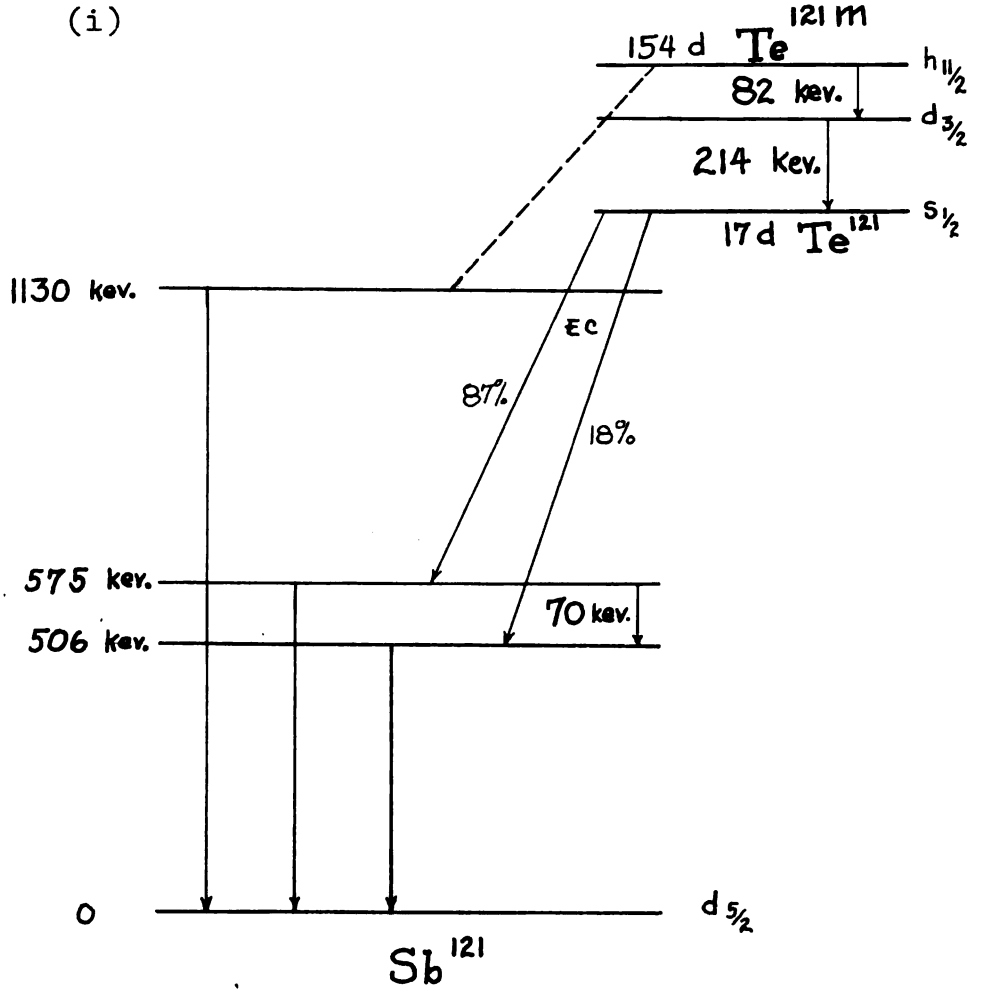

Fig. 15 Tentative Decay Scheme for Te^{121}
(From Bhatki et al.[43])

[43] Bhatki, et al., op. cit., p. 1468.

INTERNAL CONVERSION COEFFICIENTS

An excited nucleus with excitation energy less than the binding energy of any nuclear particle may de-excite by either one of two competing processes: (1) by emission of gamma rays; or (2) by internal conversion. The ratio of the transition probability of (1) to that of (2) is defined as the internal conversion coefficient (total). This total conversion coefficient is found to depend very strongly on the transition energy, the atomic number Z of the emitter, the binding energy of the shell (or subshell) from which the IC electron originated, the multipolarity L or angular momentum of the radiated field (the competing gamma emission) and the character of the nuclear transition (electric or magnetic) which in turn uniquely determines the nuclear parity change once L is fixed. It does not, however, depend on the nuclear wave function, since it is only a measure of the probabilty of one of the competing processes (as compared to the other) and not a measure of the transition probability of the nuclear decay itself. It may, however, give a clue to the nature of the electromagnetic emission.

Comparison of the theoretical (e.g., the independent-particle model) and the experimental (e.g., half-lives of gamma transitions) would allow a deduction of the multipolarities of the gamma transitions. In addition, this may give information on the angular momenta and the parities of nuclear states by direct measurements through angular correlation experiments.

To furnish the theoretical side of the comparison, the internal conversion coefficients tabulated by Rose* (for

* M. E. Rose, Internal Conversion Coefficients (North-Holland Publ. Co., Amsterdam, 1958).

the atomic numbers 42 and 51) were plotted as a function of the gamma-ray energy (in units of the electron rest-energy in Mev.). From the resulting curves, the associated internal conversion coefficients for $_{42}Mo^{96}$, $_{51}Te^{119}$ and $_{51}Te^{121}$ (for their respective gamma rays of energies up to about 200 kev.) were interpolated (the results are in Tables I to XVI, Appendix). Using the equations on p.56 (Appendix), the half-lives associated with each gamma transition (for both electric and magnetic; up to L = 3) were calculated and tabulated (See Tables XVII to XXXII, Appendix).

These theoretical estimates (Weisskopf) are to be compared with the results of angular correlation experiments in the future.

APPENDIX

Half-lives of Gamma Transitions:

Using the independent-particle model, Blatt and Weisskopf[1] arrived at expression (currently known as the Weisskopf estimate) for the (partial) half-lives of gamma transitions. These expressions have been tabulated[2] in more convenient forms (for different multipolarities) using a nuclear radius constant of 1.2×10^{-13} cm. The Table is partly reproduced here:

Half-lives of Gamma Transitions

L	$T_{1/2}$ (el)
1	$6.73\ A^{-2/3}\ E^{-3} \times 10^{-15}$ sec.
2	$9.37\ A^{-4/3}\ E^{-5} \times 10^{-9}$ sec.
3	$1.98\ A^{-2}\ E^{-7} \times 10^{-2}$ sec.
L	$T_{1/2}$ (magn)
1	$2.24\ A^{0}\ E^{-3} \times 10^{-14}$ sec.
2	$3.12\ A^{-2/3}\ E^{-5} \times 10^{-8}$ sec.
3	$6.60\ A^{-4/3}\ E^{-7} \times 10^{-2}$ sec.

[1] J. M. Blatt and V. F. Weisskopf, Theoretical Nuclear Physics (Wiley & Sons, N. Y., 1952) p.627.

[2] A. H. Wapstra, G. J. Nijgh and R. Van Lieshout, Nuclear Spectroscopy Tables (North-Holland Publ. Co., Amsterdam, 1959) p. 71.

Appendix: (Continued)

The tabulated expressions refer to the transition probability associated with the emission of multipole radiation. In order to get the actual lifetimes of the associated gamma transitions it is necessary to correct for the transition probability associated with the internal conversion process:

$$T_{\frac{1}{2}}(\gamma)^{el}_{magn} = (1 + \alpha_T)\, T^{el}_{\frac{1}{2}_{magn}} \qquad (1)$$

where α_T is the total conversion coefficient, given by:

$$\alpha_T = \alpha_K + 1.28\,(\alpha_{L_I} + \alpha_{L_{II}} + \alpha_{L_{III}}).$$

The α-subscripts refer to the particular shell (or subshell).

Appendix: (Continued)

Tables of Internal Conversion Coefficients*:

I. For Gamma Rays of Mo^{96}:

I. For the 0.216-Mev. Gamma Ray (k = 0.4227)

	a_1	a_2	a_3	β_1	β_2	β_3
K-Shell	1.18 (-2)	6.37 (-2)	2.95 (-1)	2.76 (-2)	1.52 (-1)	7.37 (-1)
L_I-Subshell	1.22 (-3)	6.50 (-3)	2.85 (-2)	3.27 (-3)	1.80 (-2)	9.90 (-2)
L_{II}-Subshell	5.00 (-5)	1.16 (-3)	1.74 (-2)	1.27 (-4)	1.27 (-3)	1.17 (-2)
L_{III}-Subshell	7.78 (-5)	1.25 (-3)	1.58 (-2)	4.20 (-5)	8.20 (-4)	1.53 (-2)
ΣL	1.35 (-3)	8.91 (-3)	6.17 (-2)	3.44 (-3)	2.01 (-2)	1.26 (-1)
$K/\Sigma L$	8.76	7.15	4.78	8.03	7.57	5.85
$\frac{L_I}{L_I}$ / $\frac{L_I}{L_{III}}$	1 / 0.0410 / 0.0638	1 / 0.1785 / 0.1923	1 / 0.6105 / 0.5544	1 / 0.0388 / 0.0128	1 / 0.0706 / 0.0456	1 / 0.1182 / 0.1545

* Interpolated from curves constructed with the values given by Rose (a's for electric, β's for magnetic; numbers in parenthesis are the powers of the factor, 10). Subscripts of the coefficients stand for the multipolarity, l. The k value stands for the gamma energy in units of the electron rest energy (in Mev.).

Appendix: (Continued)

II. For the 0.238-Mev. Gamma Ray (k = 0.466)

	a_1	a_2	a_3	β_1	β_2	β_3
K-Shell	9.10 (-3)	4.60 (-2)	2.01 (-1)	2.16 (-2)	1.13 (-1)	5.10 (-1)
L_I-Subshell	9.40 (-4)	4.63 (-3)	1.94 (-2)	2.54 (-3)	1.30 (-2)	6.55 (-2)
L_{II}-Subshell	3.60 (-5)	7.50 (-4)	1.03 (-2)	9.48 (-5)	8.85 (-4)	7.45 (-3)
L_{III}-Subshell	5.60 (-5)	8.00 (-4)	9.10 (-3)	3.34 (-5)	5.30 (-4)	8.80 (-3)
ΣL	1.03 (-3)	6.18 (-3)	3.88 (-2)	2.67 (-3)	1.44 (-2)	8.18 (-2)
$K/\Sigma L$	8.82	7.44	5.18	8.10	7.84	6.24
$\frac{L_I}{L_I}$	1	1	1	1	1	1
$\frac{L_I}{L_{II}}$	0.0383	0.1620	0.5309	0.0378	0.0681	0.1137
$\frac{L_I}{L_{III}}$	0.0596	0.1728	0.4691	0.0131	0.0408	0.1344

Appendix: (Continued)

III. For the 0.312-Mev. Gamma Ray (k = 0.611)

	a_1	a_2	a_3	β_1	β_2	β_3
K-Shell	4.37 (-3)	1.82 (-2)	6.80 (-2)	1.08 (-2)	4.60 (-2)	1.77 (-1)
L_I - Subshell	4.50 (-4)	1.86 (-3)	6.80 (-3)	1.24 (-3)	5.40 (-3)	2.17 (-2)
L_{II} - Subshell	1.42 (-5)	2.25 (-4)	2.47 (-3)	4.17 (-5)	3.33 (-4)	2.16 (-3)
L_{III} - Subshell	2.21 (-5)	2.21 (-4)	1.89 (-3)	1.44 (-5)	1.61 (-4)	2.10 (-3)
ΣL	4.86 (-4)	2.31 (-3)	1.12 (-2)	1.30 (-3)	5.90 (-3)	2.60 (-2)
$K/\Sigma L$	8.946	7.89	6.09	8.33	7.80	6.81

IV. For the 0.451-Mev. Gamma Ray (k = 0.883)

	a_1	a_2	a_3	β_1	β_2	β_3
K-Shell	1.67 (-3)	5.63 (-3)	1.68 (-2)	4.37 (-3)	1.49 (-2)	4.53 (-2)
L_I - Subshell	1.74 (-4)	5.80 (-4)	1.76 (-3)	5.00 (-4)	1.72 (-3)	5.40 (-3)
L_{II} - Subshell	4.27 (-6)	4.73 (-5)	3.80 (-4)	1.36 (-5)	8.47 (-5)	4.27 (-4)
L_{III} - Subshell	6.77 (-6)	4.20 (-5)	2.45 (-4)	5.07 (-6)	3.35 (-5)	2.97 (-4)
ΣL	1.85 (-4)	6.69 (-4)	2.39 (-3)	5.19 (-4)	1.84 (-3)	6.12 (-3)
$K/\Sigma L$	9.025	8.412	7.04	8.425	8.11	7.40

Appendix: (Continued)

V. For the 0.560-Mev. Gamma Ray (k = 1.096)

	a_1	a_2	a_3	β_1	β_2	β_3
K-Shell	9.98 (-4)	2.97 (-3)	7.78 (-3)	2.63 (-3)	7.98 (-3)	2.14 (-2)
L_I-Subshell	1.06 (-4)	3.16 (-4)	8.45 (-4)	3.01 (-4)	9.00 (-4)	2.56 (-3)
L_{II}-Subshell	2.17 (-6)	2.01 (-5)	1.34 (-4)	7.20 (-6)	3.94 (-5)	1.70 (-4)
L_{III}-Subshell	3.53 (-6)	1.70 (-5)	7.75 (-5)	2.79 (-6)	1.35 (-5)	9.98 (-5)
ΣL	1.12 (-4)	3.53 (-4)	1.06 (-3)	3.11 (-4)	9.53 (-4)	2.83 (-3)
$K/\Sigma L$	8.9346	8.411	7.364	8.457	8.374	7.56

VI. For the 0.725-Mev. Gamma Ray (k = 1.418)

	a_1	a_2	a_3	β_1	β_2	β_3
K-Shell	5.60 (-4)	1.49 (-3)	3.45 (-3)	1.45 (-3)	3.90 (-3)	9.40 (-3)
L_I-Subshell	5.85 (-5)	1.59 (-4)	3.74 (-4)	1.67 (-4)	4.45 (-4)	1.10 (-3)
L_{II}-Subshell	1.00 (-6)	7.38 (-6)	4.10 (-5)	3.54 (-6)	1.59 (-5)	5.98 (-5)
L_{III}-Subshell	1.61 (-6)	6.03 (-6)	2.11 (-5)	1.39 (-6)	4.80 (-6)	2.69 (-5)
ΣL	6.11 (-5)	1.72 (-4)	4.36 (-4)	1.72 (-4)	4.66 (-4)	1.19 (-3)
$K/\Sigma L$	9.1638	8.642	7.911	8.434	8.374	7.921

Appendix: (Continued)

VII. For the 0.770-Mev. Gamma Ray (k = 1.507)

	a_1	a_2	a_3	β_1	β_2	β_3
K-Shell	4.92(-4)	1.27(-3)	2.90(-3)	1.26(-3)	3.30(-3)	7.80(-3)
L_I-Subshell	5.25(-5)	1.35(-4)	3.13(-4)	1.43(-4)	3.77(-4)	8.97(-4)
L_{II}-Subshell	8.30(-7)	5.83(-6)	3.13(-5)	2.95(-6)	1.28(-5)	4.63(-5)
L_{III}-Subshell	1.34(-6)	4.79(-6)	1.51(-5)	1.19(-6)	3.83(-6)	2.06(-5)
ΣL	5.47(-5)	1.46(-4)	3.59(-4)	1.47(-4)	3.94(-4)	9.64(-4)
$K/\Sigma L$	8.9994	8.721	8.069	8.563	8.383	8.092

VIII. For the 0.804-Mev. Gamma Ray (k = 1.573)

	a_1	a_2	a_3	β_1	β_2	β_3
K-Shell	4.47(-4)	1.15(-3)	2.56(-3)	1.13(-3)	2.93(-3)	6.77(-3)
L_I-Subshell	4.85(-5)	1.23(-4)	2.79(-4)	1.31(-4)	3.35(-4)	7.98(-4)
L_{II}-Subshell	7.30(-7)	4.95(-6)	2.61(-5)	2.62(-6)	1.10(-5)	3.85(-5)
L_{III}-Subshell	1.19(-6)	4.07(-6)	1.32(-5)	1.07(-6)	3.38(-6)	1.69(-5)
ΣL	5.04(-5)	1.32(-4)	3.18(-4)	1.35(-4)	3.49(-4)	8.53(-4)
$K/\Sigma L$	8.8655	8.711	8.043	8.390	8.386	7.933

Appendix: (Continued)

IX. For the 0.840-Mev. Gamma Ray (k = 1.644)

	a_1	a_2	a_3	β_1	β_2	β_3
K-Shell	4.05 (-4)	1.03 (-3)	2.26 (-3)	1.02 (-3)	2.59 (-3)	5.97 (-3)
L_I-Subshell	4.45 (-5)	1.11 (-4)	2.49 (-4)	1.19 (-4)	2.97 (-4)	6.77 (-4)
L_{II}-Subshell	6.42 (-7)	4.22 (-6)	2.16 (-5)	2.32 (-6)	9.42 (-6)	2.19 (-5)
L_{III}-Subshell	1.06 (-6)	3.47 (-6)	1.09 (-5)	9.52 (-7)	2.89 (-6)	1.38 (-5)
ΣL	4.62 (-5)	1.19 (-4)	2.81 (-4)	1.22 (-4)	3.09 (-4)	7.13 (-4)
$K/\Sigma L$	8.7659	8.6781	8.0284	8.3420	8.3735	8.3766

II. For the Gamma Rays of Sb^{119}:

X. For the 0.153-Mev. Gamma Ray (k = 0.299)

	a_1	a_2	a_3	β_1	β_2	β_3
K-Shell	4.85 (-2)	2.90 (-1)	1.49 (0)	1.68 (-1)	1.17 (0)	6.30 (0)
L_I-Subshell	5.05 (-3)	2.60 (-2)	1.29 (-1)	1.82 (-2)	1.52 (-1)	1.17 (0)
L_{II}-Subshell	4.30 (-4)	1.70 (-2)	3.55 (-1)	1.09 (-3)	1.80 (-2)	1.82 (-1)
L_{III}-Subshell	6.05 (-4)	1.87 (-2)	3.35 (-1)	3.3	1.54 (-2)	4.57 (-1)
ΣL	6.09 (-3)	6.17 (-2)	8.19 (-1)	1.96 (-2)	1.85 (-1)	1.81 (0)
$K/\Sigma L$	7.970	4.700	1.819	8.574	6.311	3.483
$\frac{L_I}{L_{II}}$	1	1	0.3634	1	1	1
	0.0852	0.6538	1	0.0599	0.1184	0.1556
$\frac{L_{II}}{L_{III}}$	0.1198	0.7192	0.9437	0.0166	0.1013	0.3906

Appendix: (Continued)

XI. For the 0.270-Mev. Gamma Ray (k = 0.528)

	a_1	a_2	a_3	β_1	β_2	β_3
K-Shell	1.03 (-2)	4.38 (-2)	1.63 (-1)	3.60(-2)	1.66 (-1)	6.50 (-1)
L_I - Subshell	1.07 (-3)	4.52 (-3)	1.59 (-2)	3.97(-3)	2.10 (-2)	9.45(-2)
L_{II} - Subshell	6.56 (-5)	1.35 (-3)	1.62(-2)	2.02 (-4)	1.91 (-3)	1.30 (-2)
L_{III} - Subshell	8.55 (-5)	1.18 (-3)	1.14(-2)	5.60 (-5)	1.04(-3)	1.64(-2)
ΣL	1.22 (-3)	7.05(-3)	4.35(-2)	4.23 (-3)	2.40(-2)	1.24 (-1)
$K/\Sigma L$	8.435	6.213	3.747	8.515	6.931	5.246
$\frac{L_I}{L_{II}}$	1 / 0.0613	1 / 0.2987	0.9815 / 1	1 / 0.0509	1 / 0.0910	1 / 0.1376
$\frac{L_{II}}{L_{III}}$	0.0799 / 0.2611		0.7037 / 0.1735	0.0141 / 0.0495		

XII. For the 0.645-Mev. Gamma Ray (k = 1.262)

	a_1	a_2	a_3	β_1	β_2	β_3
K-Shell	1.18 (-3)	3.41 (-3)	8.25(-3)	4.03 (-3)	1.21 (-2)	2.95 (-2)
L_I - Subshell	1.27 (-4)	3.64 (-4)	8.99(-4)	4.65 (-4)	1.38 (-3)	3.67 (-3)
L_{II} - Subshell	3.98(-6)	3.82 (-5)	2.31 (-4)	1.71 (-5)	8.45(-5)	3.21 (-4)
L_{III} - Subshell	5.88 (-6)	2.68 (-5)	1.12 (-4)	5.00 (-6)	2.43(-5)	1.72 (-4)
ΣL	1.37 (-4)	4.29 (-4)	1.24(-3)	4.87(-4)	1.49(-3)	4.16 (-3)
$K/\Sigma L$	8.622	7.949	6.643	8.273	8.127	7.086

Appendix: (Continued)

XIII. For the 0.930-Mev. Gamma Ray (k = 1.819)

	α_1	α_2	α_3	β_1	β_2	β_3
K-Shell	5.82 (-4)	1.37 (-3)	2.98 (-3)	1.76 (-3)	4.28 (-3)	9.20 (-3)
L_I-Subshell	6.23 (-5)	1.52 (-4)	3.26 (-4)	1.89 (-4)	5.01 (-4)	1.11 (-3)
L_{II}-Subshell	1.46 (-6)	9.80 (-6)	4.64 (-5)	5.70 (-6)	2.46 (-5)	7.80 (-5)
L_{III}-Subshell	2.10 (-6)	6.10 (-6)	1.81 (-5)	1.92 (-6)	5.75 (-6)	2.73 (-5)
ΣL	6.59 (-5)	1.68 (-4)	3.90 (-4)	1.97 (-4)	5.31 (-4)	1.22 (-3)
$K/\Sigma L$	8.8369	8.160	7.631	8.951	8.056	7.570

III. For the Gamma Rays of Sb^{121}:

XIV. For the 0.070-Mev. Gamma Ray (k = 0.136)

	α_1	α_2	α_3	β_1	β_2	β_3
K-Shell	4.45 (-1)	3.50 (0)	2.15 (1)	1.50 (0)	1.90 (1)	1.65 (2)
L_I-Subshell	4.10 (-2)	3.00 (-1)	1.45 (0)	1.65 (-1)	3.15 (0)	4.50 (1)
L_{II}-Subshell	6.90 (-3)	6.80 (-1)	3.10 (1)	1.25 (-2)	3.55 (-1)	7.40 (0)
L_{III}-Subshell	9.80 (-3)	9.20 (-1)	4.00 (1)	3.30 (-3)	6.80 (-1)	4.27 (1)
ΣL	5.77 (-2)	1.90 (0)	7.245 (1)	1.808 (-1)	4.185 (0)	9.51 (1)
$K/\Sigma L$	7.712	1.842	2.968 (-1)	8.296	4.540	1.735
$\frac{L_I}{L_{II}}$	1	0.3261	0.0362	1	1	1
$\frac{L_{II}}{L_{III}}$	0.1683	0.7391	0.7750	0.0758	0.1127	0.1644
	0.2390	1	1	0.0200	0.2159	0.9489

Appendix: (Continued)

XV. For the 0.506-Mev. Gamma Ray (k = 0.99)

	α_1	α_2	α_3	β_1	β_2	β_3
K-Shell	2.13(-3)	6.45(-3)	1.70(-2)	7.40 (-3)	2.36 (-2)	6.60(-2)
L_I-Subshell	2.26 (-4)	6.85(-4)	1.88 (-3)	8.10 (-4)	2.87(-3)	8.60(-3)
L_{II}-Subshell	8.60 (-6)	9.65 (-5)	7.20(-4)	3.51 (-5)	1.96 (-4)	8.75(-4)
L_{III}-Subshell	1.18 (-5)	7.05(-5)	3.70(-4)	9.55(-6)	6.58(-5)	5.80(-4)
$\sum L$	2.46 (-4)	8.52 (-4)	2.97(-3)	8.55(-4)	3.13 (-3)	1.01 (-2)
$K/\sum L$	8.644	7.570	5.724	8.659	7.536	6.564

XVI. For the 0.575-Mev. Gamma Ray (k = 1.125)

	α_1	α_2	α_3	β_1	β_2	β_3
K-Shell	1.55(-3)	4.55(-3)	1.14(-2)	5.30(-3)	1.66(-2)	4.35(-2)
L_I-Subshell	1.66(-4)	4.84(-4)	1.28(-3)	6.01(-4)	1.98(-3)	5.50(-3)
L_{II}-Subshell	5.64(-6)	5.81(-5)	3.90(-4)	2.45(-5)	1.24(-4)	5.05(-4)
L_{III}-Subshell	8.11(-6)	4.22(-5)	1.93(-4)	6.75(-6)	3.89(-5)	3.02(-4)
$\sum L$	1.80(-4)	5.84(-4)	1.86(-3)	6.32(-4)	2.14(-3)	6.31(-3)
$K/\sum L$	8.623	7.789	6.119	8.383	7.747	6.897

Appendix: (Continued)

Tables of Half-lives of Gamma Transitions for Different Multipolarities:

1. For Mo^{96}

XVII. E = 0.216 Mev.

	$1.28(\alpha_L)$	α_T	$T_{1/2}$ (SEC.)	$T_{1/2}(\gamma)$ (SEC.)
E1	1.725 (-3)	1.352 (-2)	3.144 (-14)	3.186 (-14)
E2	1.140 (-2)	7.510 (-2)	4.215 (-8)	4.532 (-8)
E3	7.898 (-2)	3.740 (-1)	7.128 (-1)	9.794 (-1)
M1	4.402 (-3)	3.200 (-2)	2.154 (-12)	2.223 (-12)
M2	2.571 (-2)	1.777 (-1)	2.668 (-6)	3.166 (-6)
M3	1.613 (-1)	8.983 (-1)	3.604 (0)	6.842 (0)

XVIII. E = 0.238 Mev.

	$1.28(\alpha_L)$	α_T	$T_{1/2}$ (SEC.)	$T_{1/2}(\gamma)$ (SEC.)
E1	1.321 (-3)	1.042 (-2)	2.382 (-14)	2.357 (-14)
E2	7.910 (-3)	5.391 (-2)	2.790 (-8)	2.648 (-8)
E3	4.966 (-2)	2.507 (-1)	4.967 (-1)	3.971 (-1)
M1	3.415 (-3)	2.501 (-2)	1.662 (-12)	1.621 (-12)
M2	1.845 (-2)	1.315 (-1)	1.949 (-6)	1.723 (-6)
M3	1.046 (-1)	6.146 (-1)	3.470 (0)	2.149 (0)

Appendix: (Continued)

XIX. E = 0.312 Mev.

	$1.28(\alpha_L)$	α_T	$T_{1/2}$ (SEC.)	$T_{1/2}(\gamma)$ (SEC.)
E1	6.225 (-4)	4.992 (-3)	1.052 (-14)	1.057 (-14)
E2	2.952 (-3)	2.115 (-2)	7.061 (-9)	7.210 (-9)
E3	1.428 (-2)	8.228 (-2)	6.897 (-3)	7.465 (-3)
M1	1.659 (-3)	1.246 (-2)	7.285 (-13)	7.375 (-13)
M2	7.544 (-3)	5.354 (-2)	4.778 (-7)	5.033 (-7)
M3	3.323 (-2)	1.803 (-1)	4.311 (-1)	5.217 (-1)

XX. E = 0.451 Mev.

	$1.28(\alpha_L)$	α_T	$T_{1/2}$ (SEC.)	$T_{1/2}(\gamma)$ (SEC.)
E1	2.368 (-4)	1.907 (-3)	3.492 (-15)	3.499 (-15)
E2	8.567 (-4)	6.487 (-3)	1.135 (-9)	1.142 (-9)
E3	3.053 (-3)	1.985 (-2)	5.551 (-4)	5.661 (-4)
M1	6.639 (-4)	5.034 (-3)	2.430 (-15)	2.442 (-15)
M2	2.353 (-3)	1.725 (-2)	7.840 (-7)	7.975 (-7)
M3	7.839 (-3)	5.314 (-2)	3.757 (-2)	3.956 (-2)

Appendix: (Continued)

XXI. E = 0.560 Mev.

	$1.28(\alpha_L)$	α_T	$T_{1/2}$ (SEC.)	$T_{1/2}(\gamma)$ (SEC.)
E1	1.430 (-4)	1.141 (-3)	1.828 (-15)	1.828 (-15)
E2	4.520 (-4)	3.423 (-3)	3.857 (-10)	3.870 (-10)
E3	1.352 (-3)	9.132 (-3)	1.233 (-4)	1.244 (-4)
M1	3.981 (-4)	3.028 (-3)	1.272 (-13)	1.276 (-13)
M2	1.220 (-3)	9.120 (-3)	2.77 (-8)	2.702 (-8)
M3	3.622 (-3)	2.502 (-2)	8.481 (-1)	8.694 (-1)

XXII. E = 0.725 Mev.

	$1.28(\alpha_L)$	α_T	$T_{1/2}$ (SEC.)	$T_{1/2}(\gamma)$ (SEC.)
E1	7.822 (-5)	6.382 (-4)	8.418 (-16)	8.423 (-16)
E2	2.207 (-4)	1.711 (-3)	1.062 (-10)	1.064 (-10)
E3	5.582 (-4)	4.008 (-3)	2.032 (-5)	2.040 (-5)
M1	2.201 (-4)	1.670 (-3)	5.868 (-14)	5.878 (-14)
M2	5.961 (-4)	4.496 (-3)	7.396 (-7)	7.429 (-7)
M3	1.519 (-3)	1.092 (-2)	1.410 (-1)	1.426 (-1)

Appendix: (Continued)

XXIII. E = 0.770 Mev.

	$1.28(\alpha_L)$	α_T	$T_{1/2}$(sec)	$T_{1/2}(\gamma)$ (SEC.)
E1	6.998 (-5)	5.620 (-4)	7.027 (-16)	7.031 (-16)
E2	1.864 (-4)	1.456 (-3)	7.864 (-11)	7.875 (-11)
E3	4.600 (-4)	3.360 (-3)	1.334 (-5)	1.339 (-5)
M1	1.883 (-4)	1.448 (-3)	4.899 (-14)	4.907 (-14)
M2	5.038 (-4)	3.804 (-3)	5.477 (-9)	5.498 (-9)
M3	1.234 (-3)	9.034 (-3)	9.272 (-4)	9.356 (-4)

XXIV. E = 0.804 Mev.

	$1.28(\alpha_L)$	α_T	$T_{1/2}$ (SEC.)	$T_{1/2}(\gamma)$ (SEC.)
E1	6.454 (-5)	5.115 (-4)	6.176 (-16)	6.173 (-16)
E2	1.690 (-4)	1.319 (-3)	6.345 (-11)	6.337 (-11)
E3	4.074 (-4)	2.967 (-3)	9.893 (-6)	9.864 (-6)
M1	1.724 (-4)	1.302 (-3)	4.310 (-14)	4.304 (-14)
M2	4.472 (-4)	3.377 (-3)	4.430 (-9)	4.415 (-9)
M3	1.092 (-3)	7.862 (-3)	6.914 (-14)	6.860 (-4)

Appendix: (Continued)

XXV. E = 0.840 Mev.

	$1.28(\alpha_L)$	α_T	$T_{1/2}$ (SEC.)	$T_{1/2}(\gamma)$ (SEC.)
E1	5.914 (-5)	4.641 (-4)	5.413 (-16)	5.416 (-16)
E2	1.519 (-4)	1.182 (-3)	5.091 (-11)	5.097 (-11)
E3	3.603 (-4)	2.620 (-3)	7.261 (-6)	7.280 (-6)
M1	1.565 (-4)	1.176 (-3)	3.775 (-14)	3.779 (-14)
M2	3.959 (-4)	2.986 (-3)	3.548 (-9)	3.558 (-9)
M3	9.123 (-4)	6.882 (-3)	5.053 (-3)	5.088 (-3)

2. For Sb^{119}:

XXVI. E = 0.153 Mev.

	$1.28(\alpha_L)$	α_T	$T_{1/2}$ (SEC.)	$T_{1/2}(\gamma)$ (SEC.)
E1	7.789 (-3)	5.629 (-2)	7.353 (-14)	7.767 (-14)
E2	7.898 (-2)	3.690 (-1)	1.395 (-7)	1.909 (-7)
E3	1.048 (0)	2.538 (0)	2.013 (-1)	7.124 (-1)
M1	2.508 (-2)	1.931 (-1)	5.242 (-12)	6.254 (-12)
M2	2.373 (-1)	1.407 (0)	6.390 (-6)	1.538 (-5)
M3	2.316 (0)	8.616 (0)	5.975 (0)	5.745 (+1)

Appendix: (Continued)

XXVII. E = 0.270 Mev.

	$1.28(\alpha_L)$	α_T	$T_{1/2}$ (SEC.)	$T_{1/2}(\gamma)$ (SEC.)
E1	1.563 (-3)	1.186 (-2)	1.397 (-14)	1.413 (-14)
E2	9.024 (-3)	5.282 (-2)	1.060 (-8)	1.116 (-8)
E3	5.568 (-2)	2.187 (-1)	1.097 (-2)	1.337 (-2)
M1	5.412 (-3)	4.141 (-2)	1.093 (-12)	1.138 (-12)
M2	3.066 (-2)	1.967 (-1)	7.510 (-7)	8.987 (-7)
M3	1.586 (-1)	8.086 (-1)	5.960 (-1)	1.078 (0)

XXVIII. E = 0.645 Mev.

	$1.28(\alpha_L)$	α_T	$T_{1/2}$ (SEC.)	$T_{1/2}(\gamma)$ (SEC.)
E1	1.752 (-4)	1.355 (-3)	1.035 (-15)	1.037 (-15)
E2	5.491 (-4)	3.959 (-3)	1.428 (-10)	1.434 (-10)
E3	1.590 (-3)	9.840 (-3)	2.981 (-5)	3.011 (-5)
M1	6.235 (-4)	4.653 (-3)	8.309 (-14)	8.348 (-14)
M2	1.906 (-3)	1.401 (-2)	1.139 (-8)	1.155 (-8)
M3	5.329 (-3)	3.483 (-2)	2.346 (-3)	2.428 (-3)

Appendix: (Continued)

XXIX. E = 0.930 Mev.

	$1.28(\alpha_L)$	α_T	$T_{1/2}$ (sec.)	$T_{1/2}(\gamma)$ (sec.)
E1	8.430 (-5)	6.663 (-4)	3.456 (-16)	3.458 (-16)
E2	2.149 (-4)	1.585 (-3)	2.297 (-11)	2.301 (-11)
E3	4.998 (-4)	3.480 (-3)	2.326 (-6)	2.334 (-6)
M1	2.517 (-4)	2.012 (-3)	2.779 (-14)	2.785 (-14)
M2	6.800 (-4)	4.960 (-3)	1.845 (-9)	1.854 (-9)
M3	1.556 (-3)	1.076 (-2)	1.854 (-4)	1.874 (-4)

3. For Sb^{121}:

XXX. E = 0.070 Mev.

	$1.28(\alpha_L)$	α_T	$T_{1/2}$ (sec.)	$T_{1/2}(\gamma)$ (sec.)
E1	7.386 (-2)	5.189 (-1)	5.280 (-13)	8.020 (-13)
E2	2.432 (0)	5.932 (0)	1.344 (-6)	9.315 (-6)
E3	9.2736 (+1)	1.14236 (+2)	1.425 (-2)	1.642 (0)
M1	2.314 (-1)	1.731 (0)	2.391 (-11)	6.531 (-11)
M2	5.3568 (0)	2.43568 (+1)	2.993 (-5)	7.588 (-4)
M3	1.21728 (+2)	2.86728 (+2)	4.654 (-1)	1.339 (+2)

Appendix: (Continued)

XXXI. E = 0.506 Mev.

	$1.28(\alpha_L)$	α_T	$T_{1/2}$ (SEC.)	$T_{1/2}(\gamma)$ (SEC.)
E1	3.154 (-4)	2.445 (-3)	2.118 (-15)	2.123 (-15)
E2	1.090 (-3)	7.540 (-3)	4.685 (-10)	4.720 (-10)
E3	3.802 (-3)	2.080 (-2)	1.560 (-4)	1.592 (-4)
M1	1.094 (-3)	8.494 (-3)	1.714 (-13)	1.729 (-13)
M2	4.009 (-3)	2.761 (-2)	3.741 (-8)	3.845 (-8)
M3	1.287 (-2)	7.887 (-2)	1.204 (-2)	1.299 (-2)

XXXII. E = 0.575 Mev.

	$1.28(\alpha_L)$	α_T	$T_{1/2}$ (SEC.)	$T_{1/2}(\gamma)$ (SEC.)
E1	2.301 (-4)	1.780 (-3)	1.444 (-15)	1.447 (-15)
E2	7.479 (-4)	5.298 (-3)	2.478 (-10)	2.491 (-10)
E3	2.385 (-3)	1.378 (-2)	6.419 (-5)	6.507 (-5)
M1	8.093 (-4)	6.109 (-3)	1.171 (-13)	1.178 (-13)
M2	2.743 (-3)	1.934 (-2)	1.990 (-8)	2.029 (-8)
M3	8.073 (-3)	5.157 (-2)	5.046 (-3)	5.307 (-3)

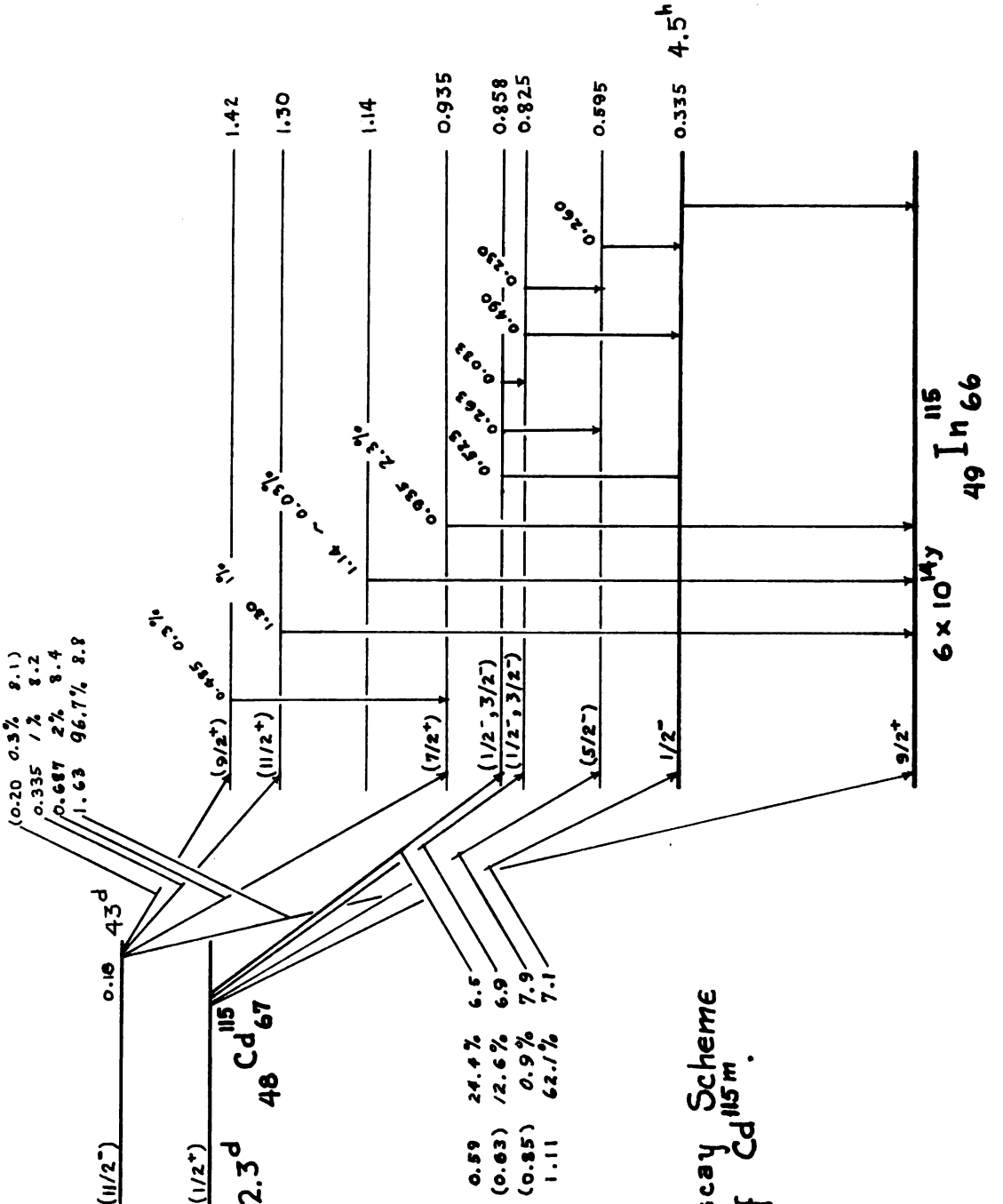

Fig. 1 Decay Scheme of Cd^{115m}.

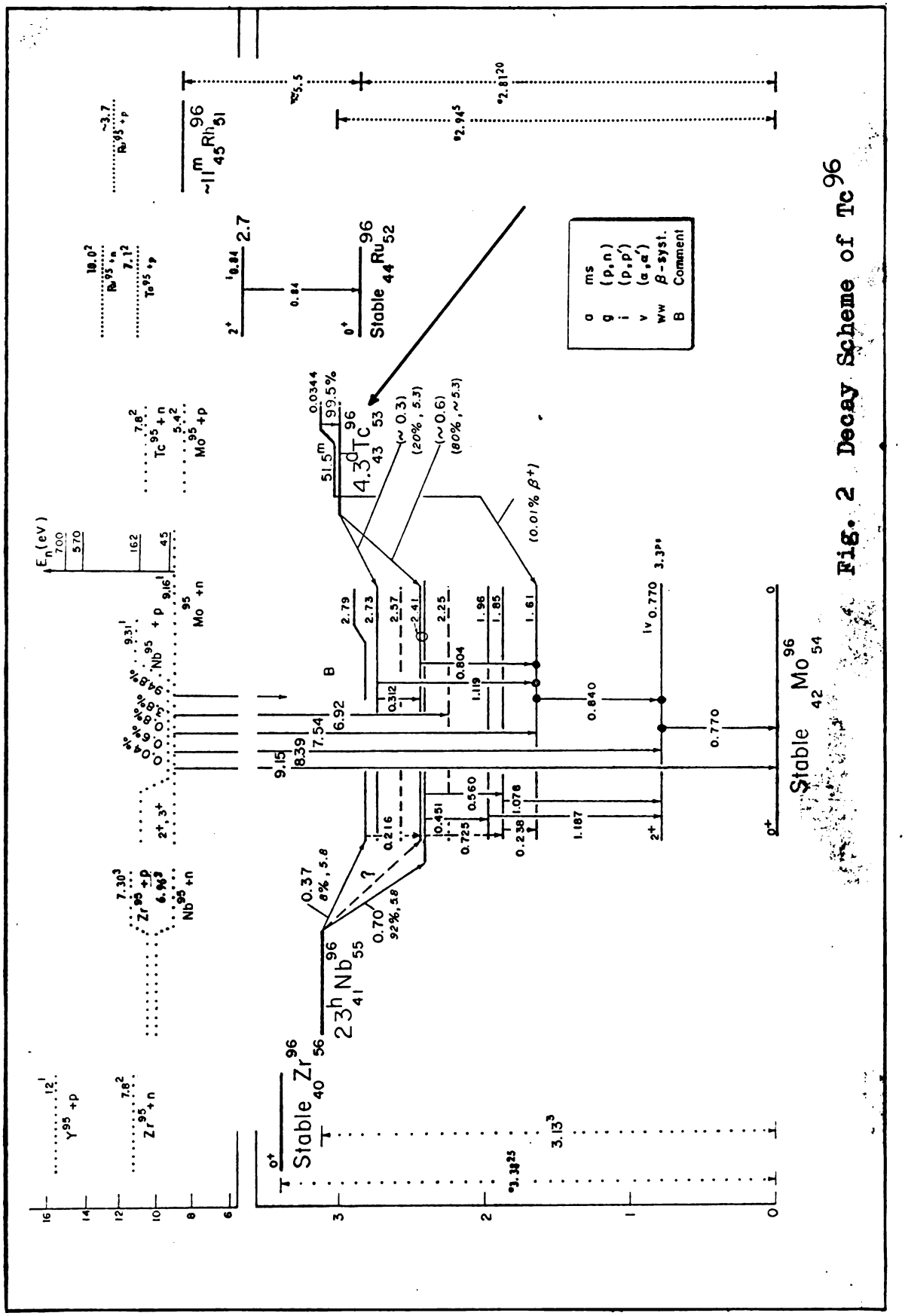

Fig. 2 Decay Scheme of Tc^{96}

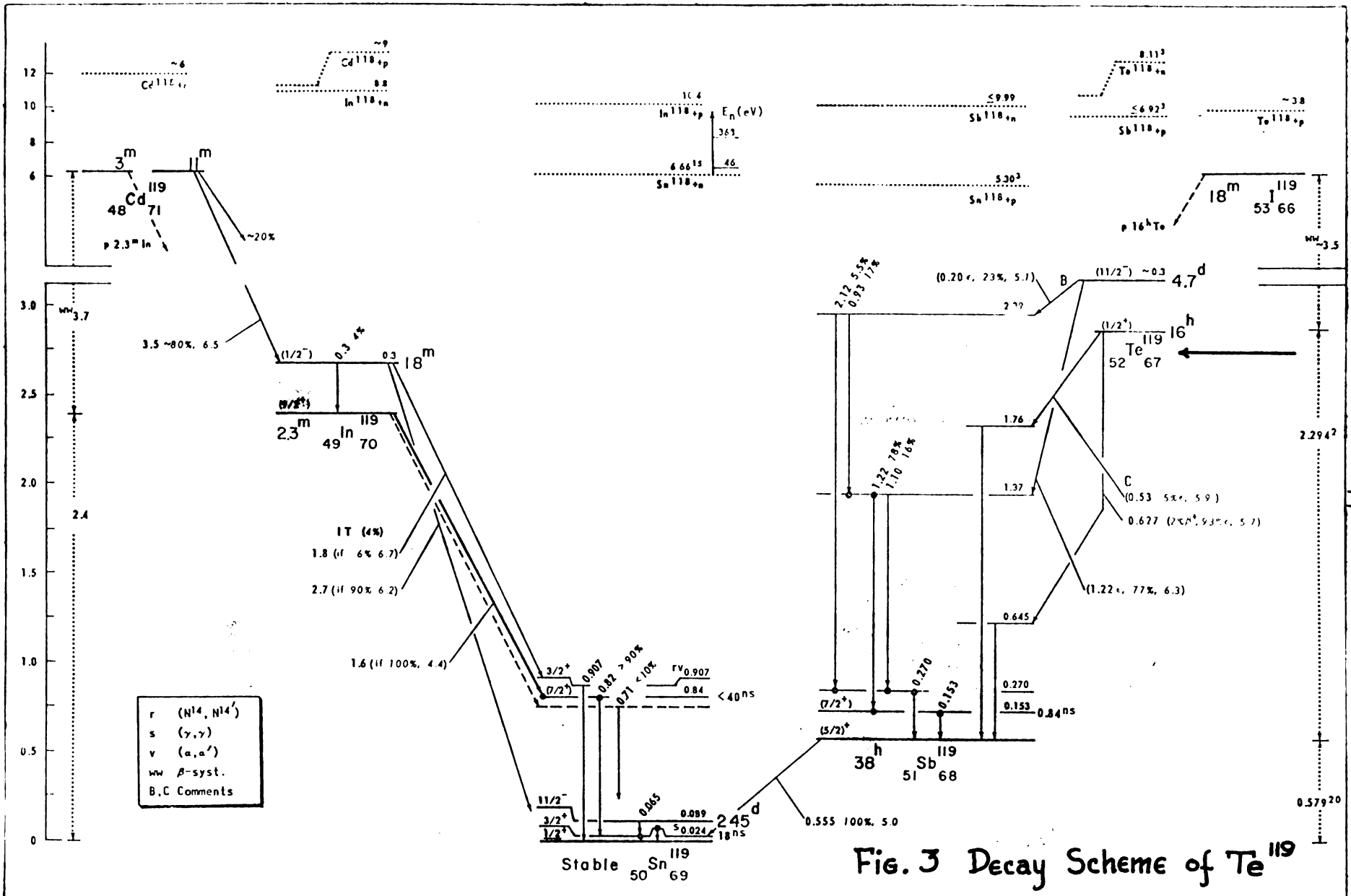

Fig. 3 Decay Scheme of Te^{119}

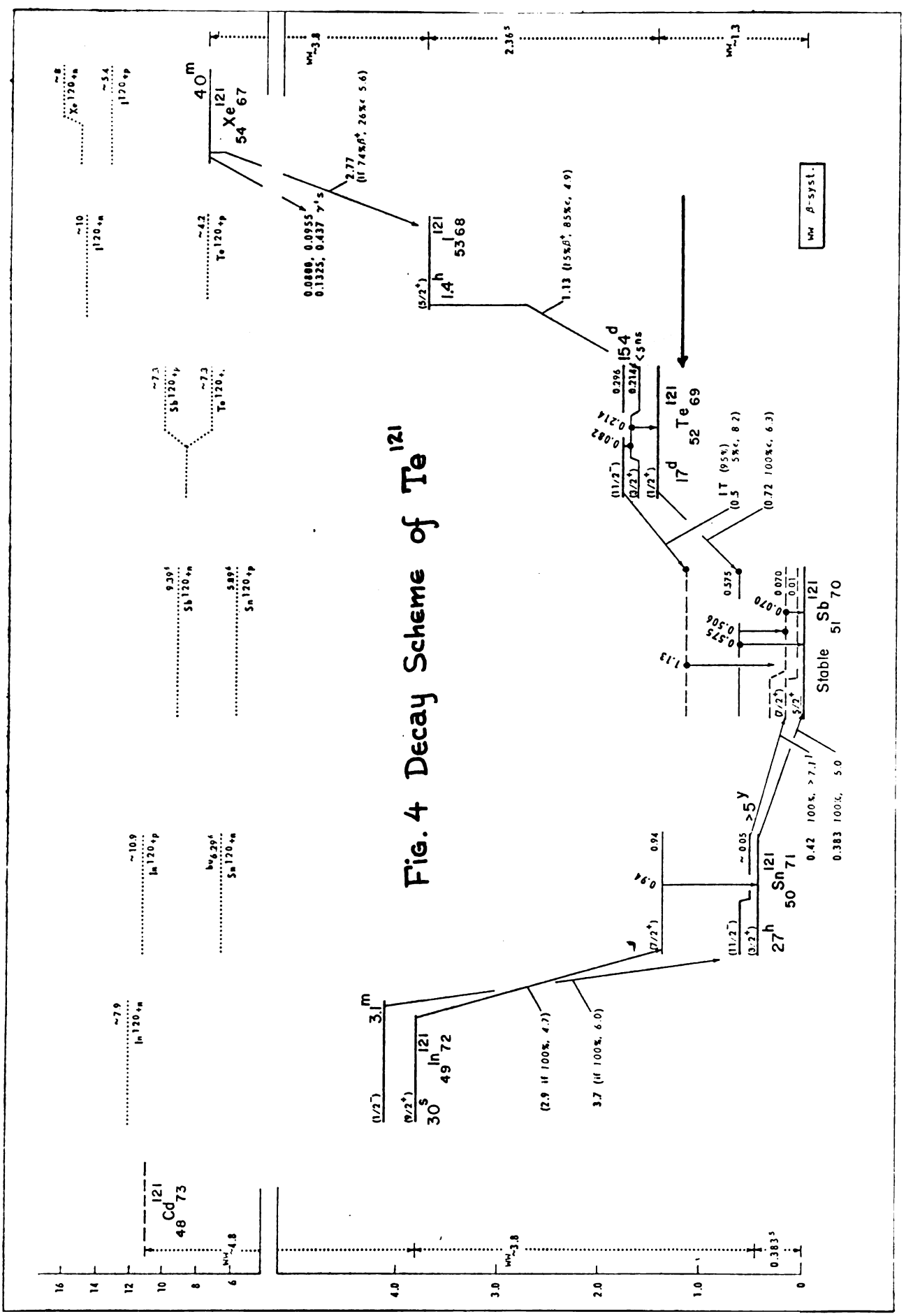
Fig. 4 Decay Scheme of Te 121
Cd 121 48 73
In 121 49 72
Sn 121 50 71
Sb 121 51 70
Te 121 52 69
I 121 53 68
Xe 121 54 67
MW β-syst.

BIBLIOGRAPHY

J. M. Blatt & V. F. Weisskopf, Theoretical Nuclear Physics (Wiley & Sons, N. Y., 1952) p. 627.

M. E. Rose, Internal Conversion Coefficients (North-Holland Publ. Co., Amsterdam, 1958).

K. Siegbahn, Beta- And Gamma-Ray Spectroscopy (North-Holland Publ. Co., Amsterdam, 1955).

A. H. Wapstra, G. J. Nijgh & R. Van Lieshout, Nuclear Spectroscopy Tables (North-Holland Publ. Co., Amsterdam, 1959) p. 71.

K. S. Bhatki, R. K. Gupta, S. Jha, & B. K. Madan, Nuovo Cimento 6: 1466 (1957).

H. Easterday & H. Medicus, Phys. Rev. 89: 752 (1953).

J. Edwards & M. Pool, Phys. Rev. 69: 140 (1946).

N. Goldberg & S. Frankel, Phys. Rev. 100: 1351 (1955).

C. W. Kocher, A. C. Mitchell, C. B. Creager & T. D. Nainan, Phys. Rev. 120: 1348 (1960).

M. Lindner & I. Perlman, Phys. Rev. 73: 1124 (1948).

M. Lindner & I. Perlman, Phys. Rev. 78: 499 (1950).

H. Medicus, A. Mukerji, P. Preiswerke & G. de Saussure, Phys. Rev. 74: 839 (1948).

K. Murakawa, Phys. Rev. 100: 1369 (1955).

T. D. Nainan, Bull. Am. Phys. Soc. 5: 239 (1960).

P. Presiwerke & Stahelin, Helv. Phys. Acta 24: 301 (1951).

G. Sprague & D. Tomboulian, Phys. Rev. 92: 105 (1953).